



UNIVERSIDADE DA BEIRA INTERIOR
Ciências

Understanding the interaction between pDNA and anion exchange supports under linear and overloaded chromatographic conditions

Patrícia Pereira Aguilar

Dissertação para obtenção do Grau de Mestre em
Biotechnologia
(2º ciclo de estudos)

Orientador: Prof. Doutora Ana Cristina Mendes Dias Cabral

Covilhã, Junho de 2014

To mum and dad

Acknowledgments

First of all I would like to thank Professor Cristina Dias-Cabral to be the responsible for my entry in the research world five years ago. Her guidance, supervision, support and encouragement were the main driving forces to this work fulfilment. And, a special thanks for her huge availability.

I also would like to thank to FCT (Portuguese Foundation for Science and Technology), project number FCOMP-01-0124-FEDER-014750 (Ref. FCT PTDC/EBB-BIO/113576/2009) and NSF (American National Science Foundation) NSF - 1246932 (award issued by CBET division of NSF), for supporting this work.

To all my family, especially mom and dad, thank you very much for the support, the encouragement words, the calls, the hugs and for tolerating my moodiness and failures as a daughter, granddaughter and sister.

For my laboratory colleagues, especially from my work group, I thank all the help and support, the work discussions, and the best breaks.

To my friends, especially from EncantaTuna, thank you for being part of my life as a family.

Last but not least, for all his love and care, support and encouragement, for being always there (tolerating all my madness), an enormous thank, with love, to Vasco.

Abstract

The potential of plasmid DNA as a therapeutic molecule in the cure of several diseases has been sustained by innumerable studies. The use of pDNA in therapies (DNA Vaccines and Gene Therapy) requires its production at the gram scale, with high purity levels and in an economic way, always taking into account the guidelines from the regulatory agencies. Anion-exchange chromatography have been successfully used in pDNA purification. Nevertheless, the mechanism of pDNA separation using this technique is still not completely understood. Additionally, due to economic reasons, it may be interesting to run the chromatographic processes in the overloaded mode. However, the overloaded mode is considerably more complex than linear chromatography, and suitable models do not exist. Thus, the prediction of separation behavior is generally unreliable, being a major impediment in the design and implementation of scaled-up units. Therefore, a better understanding of the mechanisms underlying non-linear chromatography of biomolecules has considerable practical interest.

Flow Microcalorimetry (FMC) has proven its ability to provide an improved understanding of the driving forces, mechanisms and kinetics involved in the adsorption process of biomolecules onto several chromatographic systems. Thus, using FMC as a central technique, this study aims to understand the adsorption mechanism of pDNA (pVAX1-LacZ) onto the anion-exchange support Fast Flow Q-sepharose, considering linear and overloaded conditions and showing the role of nonspecific effects at the adsorptive process. Static binding capacity, Isothermal Titration Microcalorimetry (ITM) and fast performance chromatography were also accomplished to obtain a better understanding of the adsorption mechanism. Static binding capacity studies revealed that the mechanism of pDNA adsorption onto Q-sepharose follows a Langmuir-type isotherm profile. FMC experiments were performed in the linear, transition and overloaded zones of the isotherm, through a pulse injection or a continuous feed. All obtained thermograms comprised a first endothermic peak followed by an exothermic peak which, in some cases (volume overloading), resulted from overlapped peaks. Endothermic heat major contributor was suggested to be the desolvation process. Exothermic heats were related to the interaction between pDNA and Q-sepharose primary and secondary adsorption. Furthermore, FMC revealed that the overall adsorption process is exothermic, as expected for an anion-exchange interaction. Nevertheless, there are evidences of the presence of nonspecific effects, such as reorientation and electrostatic repulsive forces.

Key words

Flow Microcalorimetry; Isotherms; Adsorption; Plasmid DNA; Anion Exchange Chromatography.

Resumo alargado

O elevado potencial da utilização de moléculas de DNA, na forma de plasmídeos, em terapias cujo objetivo é o tratamento ou a cura de várias doenças, tem sido comprovado por inúmeros estudos desenvolvidos recentemente. No entanto, a utilização deste tipo de moléculas em terapias como Vacinas de DNA e na Terapia Génica, exige que a sua produção seja realizada até se atingir a escala da grama e garantindo elevados níveis de pureza do plasmídeo. Para além disso, pretende-se que o processo seja realizado da forma mais económica possível, cumprindo sempre as diretrizes das agências reguladoras como por exemplo a FDA (*Food and Drug Administration*) e a EMEA (*European Agency for the Evaluation of Medical Products*).

Vários processos têm sido utilizados no processo de purificação de plasmídeos, quer para a sua separação de impurezas como restos celulares, proteínas, DNA genómico, etc., quer para separar as diferentes isoformas em que um plasmídeo se pode encontrar (linear, circular aberto ou superenrolado). Uma das técnicas que tem sido utilizado com sucesso é a cromatografia de troca aniónica. No entanto, o mecanismo de separação de plasmídeos por esta técnica não é, ainda, totalmente compreendido. Para além disso, devido a razões económicas, sugere-se que os processos cromatográficos sejam conduzidos em modo de sobrecarga, ou seja através da sobrecarga da coluna de cromatografia. Contudo, trabalhar em sobrecarga é consideravelmente mais complexo do que trabalhar em cromatografia linear e, até ao momento, não existem modelos adequados que prevejam o mecanismo do processo cromatográfico nestas condições. Deste modo, a previsão do comportamento das moléculas neste caso, bem como do resultado da separação através de cromatografia não é viável, sendo um dos principais obstáculos na conceção e implementação de unidades preparativas à escala industrial. Assim, uma melhor compreensão dos mecanismos subjacentes à cromatografia não linear tem um elevado interesse prático.

A análise termodinâmica dos processos de adsorção através da Microcalorimetria de Fluxo (FMC) tem vindo a ser utilizada para obter uma melhor compreensão das forças motrizes, dos mecanismos e das cinéticas envolvidas no processo de adsorção de biomoléculas em diferentes sistemas cromatográficos. Por isso, neste trabalho, através da utilização da microcalorimetria de fluxo, pretende-se compreender o mecanismo de adsorção de um plasmídeo na sua forma linear (*ln pVAX1-LacZ*) sobre um suporte cromatográfico de troca aniónica (*Fast Flow Q-sepharose*). Os ensaios foram levados a cabo de modo a que o processo possa ser avaliado em condições lineares e em condições de sobrecarga. Para além do estudo do processo de adsorção tendo em conta a interação entre a biomolécula e o suporte cromatográfico, foi também considerada e avaliada a presença e a influência de efeitos não específicos como por exemplo a reorientação da biomolécula. Para além da microcalorimetria de fluxo, para obter uma

melhor compreensão do mecanismo de adsorção, foram também realizados estudos da capacidade de ligação em modo estático (*static binding capacity*), microcalorimetria de titulação (*Isothermal Titration Microcalorimetry*) bem como estudos cromatográficos (*fast performance chromatography*). Os resultados obtidos nos estudos de capacidade de ligação revelaram que o processo de adsorção do plasmídeo segue uma isotérmica de Langmuir, em que a capacidade de ligação da Q-sepharose aumenta com o aumento da concentração de plasmídeo em equilíbrio até se atingir um patamar em que a saturação do suporte cromatográfico é atingida. Os estudos realizados utilizando a microcalorimetria de fluxo foram efetuados nas zonas linear, de transição e de sobrecarga tendo em conta a isotérmica construída. A injeção das amostras foi realizada de dois modos diferentes, através da introdução de um pulso de amostra na célula do microcalorímetro ou através da alimentação contínua de amostra na célula. Estes modos de injeção foram conseguidos utilizando *loops* de diferentes volumes. Todos os termogramas obtidos são compostos por um primeiro pico endotérmico seguido de um pico exotérmico, o qual, em alguns casos específicos (sobrecarga de volume) resulta de picos sobrepostos. Para os picos endotérmicos o processo de dessolvatação foi sugerido como sendo o principal contribuinte enquanto que para o caso dos picos exotérmicos a interação entre o DNA e o suporte cromatográfico e a adsorção secundária foram apontados como os principais contribuidores. Para além disso, a microcalorimetria de fluxo sugere que o processo global de adsorção é exotérmico, o que é esperado uma vez que se trata de uma interação de troca aniónica. No entanto, foram também demonstradas evidências da presença de efeitos não específicos do processo de adsorção, nomeadamente a reorientação e a repulsão electrostática entre as moléculas adsorvidas.

Palavras-chave

Microcalorimetria de Fluxo; Isotérmica; Adsorção; Plasmídeo; Cromatografia de troca aniónica.

Index

1.	Introduction-----	1
1.1.	Plasmid DNA (pDNA) -----	1
1.1.1.	pDNA as a therapeutic molecule (Gene Therapy and DNA Vaccines)---	1
1.1.2.	DNA composition and properties -----	4
1.2.	Plasmid DNA biotechnological manufacture-----	7
1.2.1.	Upstream processing - pDNA production -----	8
1.2.2.	Downstream processing - pDNA recovery/isolation-----	9
1.2.3.	Downstream processing - pDNA purification -----	10
1.3.	Ion Exchange Liquid Chromatography -----	13
1.3.1.	Anion Exchange Chromatography (AEC) in pDNA purification -----	14
1.4.	Static Binding Capacity-----	15
1.5.	Thermodynamic analysis of biomolecules adsorption -----	18
1.5.1.	Microcalorimetry: Flow (FMC) and Isothermal Titration (ITM)-----	18
1.6.	Goal of Study-----	23
2.	Material and Methods -----	25
2.1.	Materials -----	25
2.2.	Apparatus and software-----	26
2.3.	Plasmid DNA production -----	26
2.3.1.	Fermentation -----	26
2.3.2.	Recovery and Purification-----	26
2.3.3.	Agarose Gel Electrophoresis -----	28
2.3.4.	Plasmid DNA digestion -----	28
2.3.5.	Plasmid DNA quantification -----	28
2.4.	Adsorption Isotherms -----	28
2.5.	Flow Microcalorimetry (FMC)-----	29
2.6.	Isothermal Titration Microcalorimetry (ITM) -----	30
2.7.	Fast performance chromatography -----	30
3.	Results and Discussion -----	32
3.1.	Plasmid DNA production -----	32
3.2.	Static Binding Capacity-----	33
3.3.	Flow Microcalorimetry (FMC)-----	35
3.4.	Isothermal Titration Microcalorimetry (ITM) -----	49
4.	Conclusions and future work-----	51
	References -----	54

1. Introduction

1.1. Plasmid DNA (pDNA)

1.1.1. pDNA as a therapeutic molecule (Gene Therapy and DNA Vaccines)

The potential of plasmid DNA (pDNA) as a therapeutic molecule in the cure of several diseases has been sustained by innumerable recent studies (Ghanem et al., 2013; Ginn et al., 2013; Li et al., 2012; Sousa et al., 2009). More than a successfully applied method to animal models in the prevention or treatment of infectious diseases, cancer, autoimmunity and allergies (Li et al., 2012), the use of pDNA vectors instead of the pathogens or its proteins offers more convenient development and production strategies. Using a generic method based on bacterial cultures and DNA preparation protocols, it's possible to produce pDNA in a less expensive and easier way (Sousa et al., 2009). Furthermore, these strategies have a safer profile once they avoid the need to directly handle with dangerous organisms.

Up to the year of 2013, more than 1800 clinical trials in gene therapy have been completed, are ongoing or have been approved worldwide, **Figure 1.1.1.1**. In its majority (81.3%) gene therapy clinical trials were addressed to cancer, monogenic diseases and infectious diseases, **Figure 1.1.1.2** (Ginn et al., 2013).

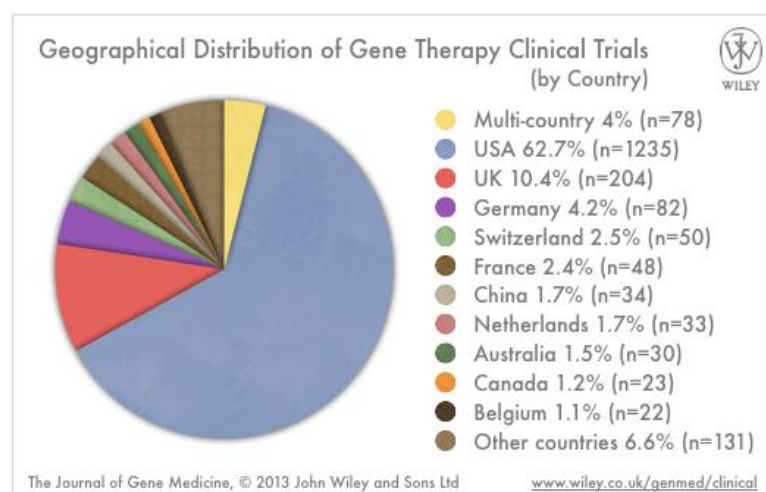


Figure 1.1.1.1 - Geographical distribution of gene therapy clinical trials.

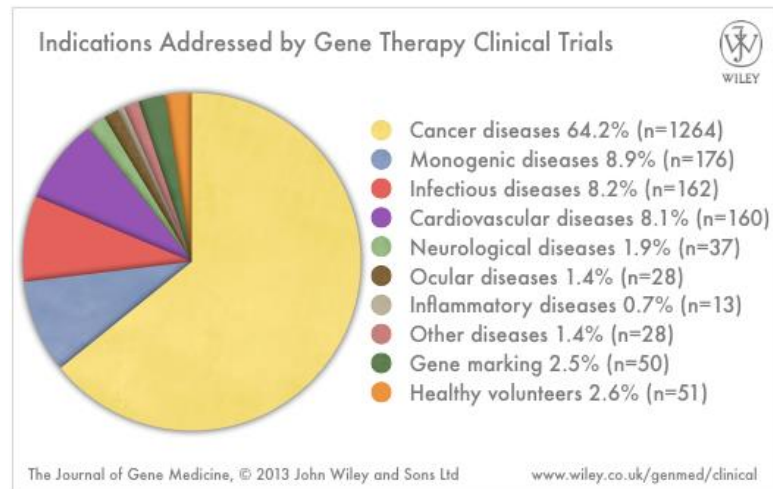


Figure 1.1.1.2 - Indications addressed by gene therapy clinical trials.

A range of different vectors have been used in gene therapy trials, **Figure 1.1.1.3**. Owing to safety concerns and the relatively small therapeutic capacity of DNA viral vectors, the development of nonviral vectors has been increasing over the years. “Naked DNA” or pDNA is the simplest and most popular nonviral system (Ginn et al., 2013).

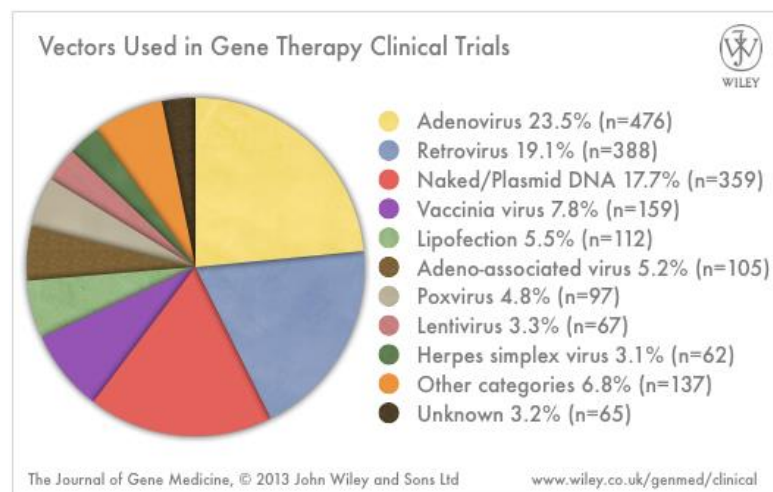


Figure 1.1.1.3 - Vectors used in gene therapy clinical trials.

The use of genes themselves as drugs to treat diseases requires efforts of researchers to develop efficient technologies to produce them at the gram scale, with high purity levels and in an economic way. Furthermore, plasmid-based gene therapy drugs require rigorous in-process and

end-product characterization as they have been included in the list of “well-characterized” biotechnology products (Kelly, 2003). Thus, all the production, recovery and purification steps have to be carried out according to regulatory agencies guidelines, such as FDA (Food and Drug Administration) and EMEA (European Agency for the Evaluation of Medical Products), and also performed under current “Good Manufacturing Practices” (cGMP) (Sousa et al., 2009).

Gene therapy and DNA vaccines are plasmid-mediated therapies which principle is based on the administration to a patient of a genetic engineered DNA molecule (for example pDNA) carrying a “medicinal gene”. In gene therapy, the medicinal gene may code either for a missing or defective protein or may be antigenic (DNA vaccines) (Kelly, 2003). Therefore, gene therapy has the potential to cure or reverse genetic diseases. Beyond that, DNA vaccines, as the conventional ones, aim to confer long-term protection against infectious diseases. In this circumstance, pDNA is genetically engineered to produce specific proteins, from a disease causing pathogen, that act like antigens. Within the cell, pDNA is converted into pathogenic proteins using the “inner machinery” of the host cell. After that, these proteins are recognized as foreign, processed by the host cell and exposed to the immune system of the organism (Ghanem et al., 2013). At these stage, DNA vaccines have the ability to triggering both humoral and cellular immune responses (Sousa et al., 2009).

Despite the success in veterinary applications, human DNA vaccines still have to overcome some challenges (**Table 1.1.1.1**) that arose from the clinical trials already performed. Nevertheless, positive facts have also arisen in these trials and encourage researchers to conduct efforts for increasing the efficacy of DNA vaccines hoping to achieve regulatory approval and commercial exploitation.

Table 1.1.1.1 - Advantages and disadvantages of DNA vaccines.

Advantages	Disadvantages
<ul style="list-style-type: none"> - DNA is inexpensive compared to isolated proteins or organisms used for conventional vaccines - DNA vaccines can result in longer lasting producing of the antigenic protein; thereby booster shots are no longer required - Produces stronger immune response than conventional vaccines - Stability of vaccine for storage and shipping - Easy development and production - Subunit vaccination with no risk for infection 	<ul style="list-style-type: none"> - Testing results have been favorable in small animals, but less impressive in larger ones (including humans) - DNA uptake to cells apparently decreases with increased body size - Extended immunostimulation could lead to chronic inflammation or autoantibody production - Limited to protein immunogens (not useful for non-protein based antigens such as bacterial polysaccharides) - Risk of affecting genes controlling cell growth
(Ghanem et al., 2013)	

Therefore, large scale plasmid DNA manufacturing processes must continue to be developed and optimized as gene therapy and DNA vaccines move from research laboratories to clinical and market approval.

1.1.2. DNA composition and properties

Deoxyribonucleic acid, DNA, is a nucleic acid polymer in which the repeating units are nucleotides. These comprise a nitrogenous base, a five carbon sugar and a phosphate group, **Figure 1.1.2.1**. In DNA there are two groups of nucleotides according to its nitrogenous base. Adenine and Guanine belong to purine bases while Thymine and Cytosine to pyrimidine bases. Due to their unique structures, Adenine always pairs with Thymine whereas Guanine pairs with Cytosine, **Figure 1.1.2.2**. At pH greater than 4, unbound phosphate groups are ionized and each nucleotide contributes with a negative charge to the overall net charge of the DNA molecule. Thus, nucleic acids are polyanionic molecules (Ferreira, 2005).

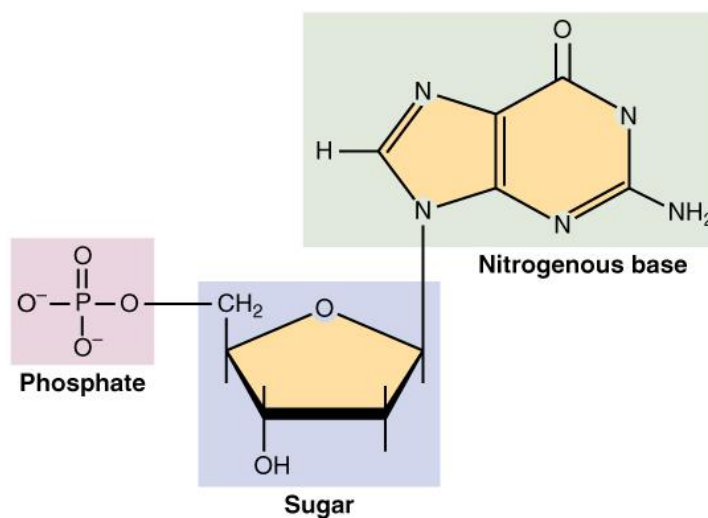


Figure 1.1.2.1 - Nucleotide (adapted from www.openstaxcollege.org, accessed in 14/01/2014).

To form a DNA strand, nucleotides are linked through phosphodiester bounds between the hydroxyl group of the 3' sugar carbon of a nucleotide and the phosphate group of the 5' sugar carbon of the adjacent nucleotide. The winding of two antiparallel DNA strands, connected through hydrogen bounds between complementary nucleotides in each strand, results in the right-handed double helix structure, **Figure 1.1.2.2** (Ferreira, 2005).

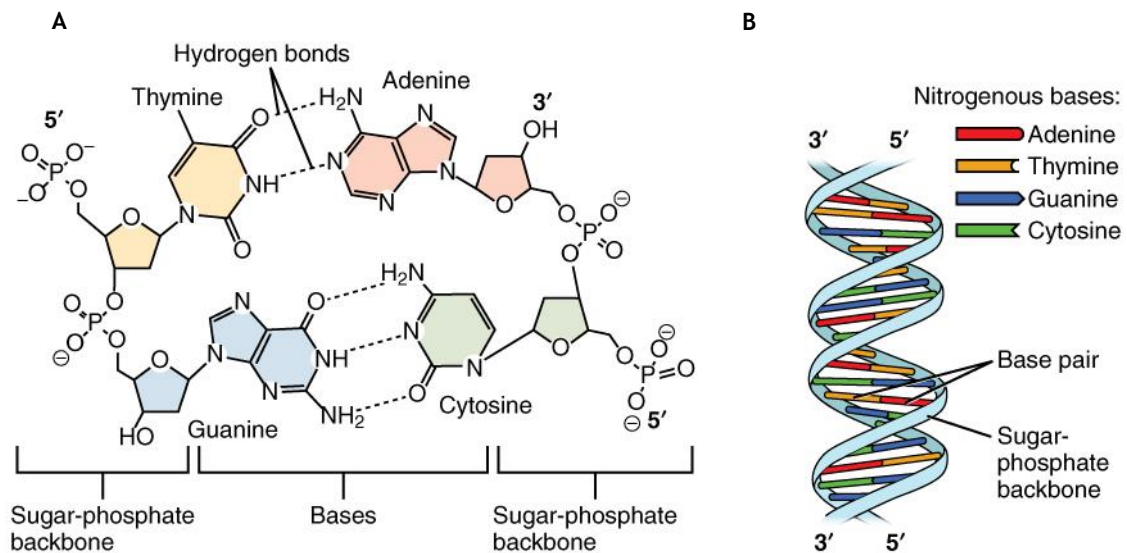


Figure 1.1.2.2 - A - Antiparallel DNA strands connected through hydrogen bonds between complementary nucleotides; B - DNA right-handed double helix (adapted from www.openstaxcollege.org, accessed in 14/01/2014).

Plasmids are high molecular weight ($M > 10^6$ Da), double-stranded DNA molecules in which the two ends of the DNA strands are covalently linked, forming a closed loop, **Figure 1.1.2.3**. In nature, plasmids are part of the bacterial genome but located separately from its chromosomal DNA. Within the bacteria, pDNA codes only for some specific functions (example: antibiotic resistance) and can be replicated independently of chromosomal DNA where all the essential functions are present (Ghanem et al., 2013; Sousa et al., 2009).

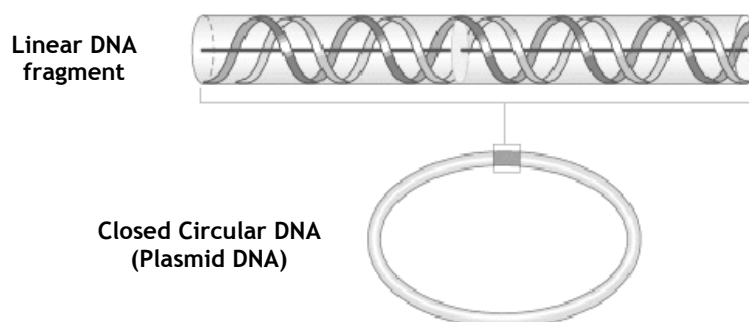


Figure 1.1.2.3 - Plasmid DNA (adapted from Ferreira, 2005)

In a wide range of biological processes, such as transcription, replication, recombination, control of gene expression and genome organization, DNA topological conformation is of fundamental importance. DNA plasmids can exist in three types of conformations which are supercoiled (sc), open circular (oc) and linear (ln) **Figure 1.1.2.4**. The more complex and biologically active form is supercoiled pDNA, also known as closed circular DNA. If one strand of sc pDNA is nicked the supercoiling is loosed, resulting in the open circular conformation. Furthermore, if both strands are cleaved, approximately in the same position, linear conformation is generated (Sousa et al., 2009).

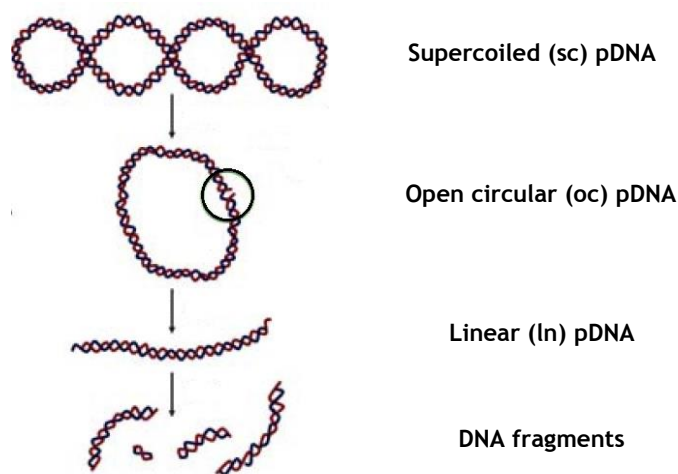


Figure 1.1.2.4 - Plasmid DNA topological conformations (adapted from (Fernández et al., 2011))

Plasmid DNA has become very promising in gene therapy strategies, once it has already demonstrated biological activity in humans and it can be genetically manipulated, produced by non-complex cultivation of *Escherichia coli* (*E. coli*) and purified in subsequent downstream processes. Therefore, it is important to develop and optimize all the processes to produce pure supercoiled plasmid DNA.

1.2. Plasmid DNA biotechnological manufacture

The increased interest in using pDNA in a wide range of gene therapies and DNA vaccines, did arise the need to produce considerable amounts (gram scale / industrial processes) of pharmaceutical grade pDNA.

The biotechnological manufacture of pDNA can be separated in two stages, the upstream and the downstream processing. The upstream processing involves the steps in which the pDNA is produced by cells genetically engineered to contain the gene of interest. Then, the downstream processing aims to isolate and purify the pDNA (Sousa et al., 2009). Either for laboratory scale or for industrial scale, **Figure 1.2.1** outlines the schematic process steps for the development of pDNA. Generally this process starts with the selection and construction of appropriate expression vectors and production microorganisms. Then, the fermentation conditions are selected and optimized, allowing cell growth and pDNA production. Finally, pDNA is isolated and purified (Ferreira et al., 2000b).

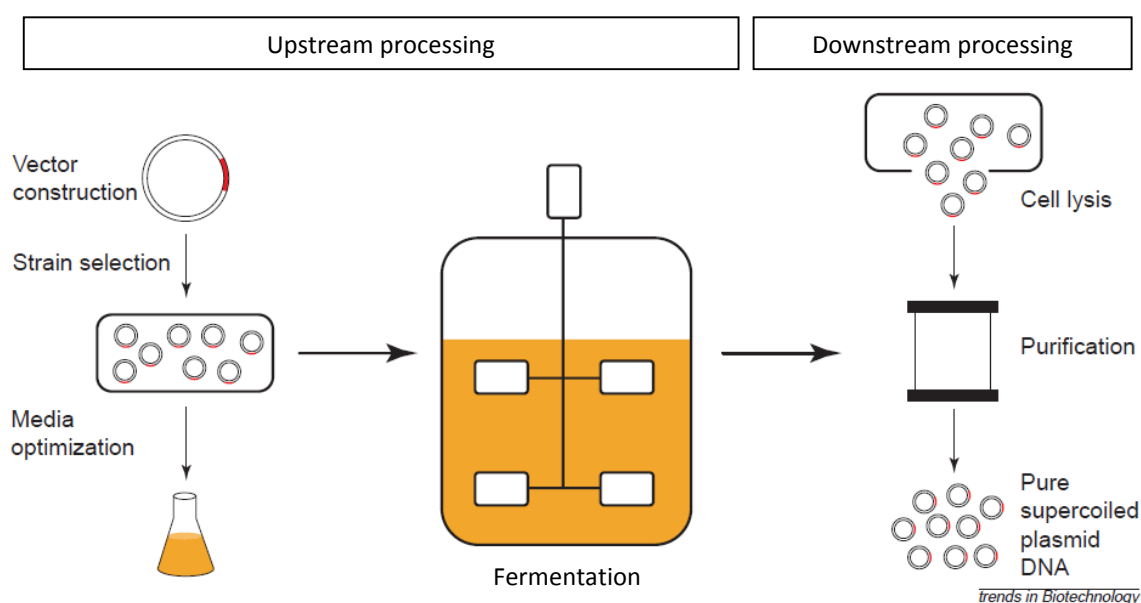


Figure 1.2.1 - Schematic process steps for the development of plasmid DNA (adapted from (Ferreira et al., 2000b))

The production and the quality of a biotechnological product is determined either by the up and the downstream processing. Thus, all manufacturing processes for the production of pDNA must be previously designed in detail and then controlled at each phase.

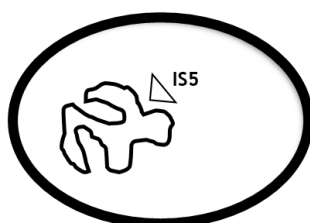
1.2.1. Upstream processing - pDNA production

The manufacturing process for pDNA production starts with the construction of the vector. This consists of a plasmid backbone that includes typical elements as the origin of replication (for plasmid replication in the cell), an antibiotic resistance gene (for cells to grow under selective pressure in a media containing the encoded antibiotic), a stronger eukaryotic promoter (to stimulate the transcription of the pDNA in the eukaryotic cells), and poliadenylation signal sequence (part of the process that produces mature mRNA for translation in eukaryotic cells). Moreover, the vector encodes the therapeutic gene(s) (Sousa et al., 2009).

Succeeding its construction, the vector must be inserted in bacterial cells in order to create a uniform inoculum for further production and large scale fermentation. Biomass productivity, plasmid yield, plasmid quality and manufacturing costs may be improved through the optimization of the biological system, growth environment and growth conditions. Since open circular and linear pDNA isoforms are difficult to remove during the purification processes and are considered undesirable by regulatory agencies, plasmid fermentation processes are optimized to maximize both the volumetric (biomass concentration) and specific (pDNA copy number) yields of high quality supercoiled plasmid. Furthermore, high volumetric yields enable smaller and economical fermentations and high specific yields increase plasmid purity leading to easier and reliable economic downstream processes. To achieve high quality and high yields, plasmid fermentations need to use reduced growth rates as high ones have been associated with acetate production, plasmid instability and lower percentages of supercoiled plasmid. (Sousa et al., 2009).

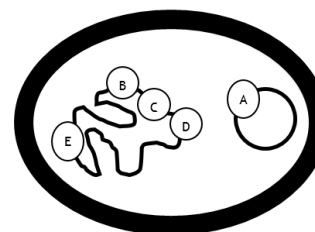
Another key factor to be considered for pDNA fermentations is the bacterial host. Typically, pDNA is manufactured using *E. coli* K12 attenuated strain, **Figure 1.2.2.**, which is considered “automatically exempt” by NIH (National Institutes of Health) because is nonpathogenic and have limited survival if released to the environment (Sousa et al., 2009). Beyond that, recombinant *E. coli* strains are known for being easy to produce and are industrially important because of their well characterized genetics and cellular metabolism (Silva et al., 2009).

E. coli K-12



- no toxins
- no adhesion factors
- no invasion factors
- no iron-transport systems
- no capsule
- no plasmids
- smaller genome
- rough colony type (partial LPS)

Pathogenic *E. coli*



- A - iron transport
- B - toxins
- C - capsule
- D - adhesion factors
- E - invasion

Figure 1.2.2 - Comparison of *E. coli* K12 strain and pathogenic *E. coli*

Likewise essential is the medium used in the fermentation process. Fermentation medium must supply adequate quantities of nutrients needed for energy, biomass and cell maintenance. In particular, the medium should support high nucleotide pools and supply energy for plasmid replication while minimizes other cell activities and overproduction of contaminants (Sousa et al., 2009).

After a fermentation process, cells are removed from the slurry through a centrifugation step and then they can be stored (-20°C) or the process can progress to the downstream processing where pDNA will be recovered and isolated from the cells and finally purified according to the regulatory agencies guidelines.

1.2.2. Downstream processing - pDNA recovery/isolation

Following the upstream processing, the downstream aims to recovery, isolate and purify the pDNA, specially the supercoiled isoform (Sousa et al., 2009). Generally, the separation and purification of biomolecules are technically challenging processes since all biomolecules of interest are labile. Furthermore, pDNA recovery and purification are problematic due to the similar structural nature of the contaminants and the pDNA. These similarities include size, shape and conformation, rheological properties (e.g. viscosity) of the lysates and process streams, as well as structural and chemical properties like negative charge (RNA, gDNA, endotoxins) or hydrophobicity (endotoxins) (Ghanem et al., 2013).

Fermentation is usually optimized in order to obtain high cell density and high plasmid copy number, after that, a cell lysis step is performed to recover pDNA from the cells. Due to the release of cell components regarded as contaminants (gDNA, RNA, proteins and endotoxins) during the lysis step, a sequence of downstream processing operations has to be done to obtain a final preparation with pDNA purity levels according to the regulatory agencies guidelines for therapeutic usage (homogeneous preparation of sc pDNA >97%). Taking into account the global process of pDNA (and other biomolecules) production, downstream operations have significant relevance and are considered the most important and expensive ones (Sousa et al., 2009).

Thus, after the fermentation step, to eliminate contaminants and until achieve a suitable purity degree of supercoiled pDNA, several unit operations must be performed, such as cell harvest, lysis, cell debris solid separation, affinity precipitation, adsorption, buffer exchange and concentration (Ferreira et al., 2000b; Ghanem et al., 2013).

Considering its intracellular nature, to recover pDNA from the cells after fermentation, some degree of lysis or cell breakage is required first. This leads to the release of all the intracellular components, including pDNA, RNA, gDNA, proteins and endotoxins (Ferreira et al., 2000b). In the last years, efforts have been made to optimize lysis and further recovery of pDNA in order to maximize purity levels at harvest. Variations of the alkaline lysis protocol, originally described by Birnboim and Doly (1979) and adapted by Lahijani and co-workers (1996), have been the procedure of choice for cell disruption to recover pDNA (Sousa et al., 2009). The protocol used in this study is explained later in “Material and Methods” section. The use of this method has gained interest over the years once it allows the removal of host cell’s gDNA and proteins through denaturation and further selective precipitation. However, the final lysate still contain significant amounts of proteins, RNA and endotoxins, requiring subsequent steps in the downstream process to separate them from pDNA. Clarification and concentration steps are performed in order to remove these impurities and simultaneously reduce the volume of the samples for the final purification and polishing steps (Ferreira et al., 2000b; Sousa et al., 2009).

Therefore, recovery/isolation it’s a process of capturing, concentrating and mild purify supercoiled pDNA. This has to be a high throughput process to avoid product degradation and maximize product yield (Ghanem et al., 2013).

1.2.3. Downstream processing - pDNA purification

As previously mentioned, pDNA purification has specific concerns due to its structural nature (size, shape and conformation), as well as due to the presence of impurities with similar physicochemical properties and that behave identically in the majority of the operations (Ferreira, 2005; Ghanem et al., 2013). The purification strategy of pDNA follows, as well as the purification of other biomolecules, general rules that dictate that along the process unit operation capacity decreases as resolution increases (Ferreira, 2005).

Within some options as ultrafiltration, precipitation or two-phase systems, liquid chromatography is undoubtedly the central technique used to purify supercoiled pDNA from its other isoforms and from related impurities including remaining gDNA, RNA, proteins and endotoxins (Ferreira, 2005; Sousa et al., 2009). In chromatographic methods, nucleic acid capture onto absorbents is affected by the size, the base composition, the secondary structure and the conformation of the nucleic acids. Additionally, the capacity of the absorbent is another parameter to consider in pDNA purification.

Different pDNA properties such as size, charge, hydrophobicity, accessibility of the nucleotide bases residing within single or double stranded nucleotide acid molecules, and the topological constraints due to supercoiling, have been exploited in the understanding of the interactions between nucleic acids and supports used in chromatography to separate sc pDNA from its topoisomers and from related impurities such as gDNA, RNA and endotoxins (Ferreira, 2005). Thus, several chromatography techniques have been applied, such as size-exclusion, ion-exchange, hydrophobic interaction and affinity chromatography (Table 1.2.3.1). These methodologies may be applied either isolated or within an overall purification strategy (Ghanem et al., 2013; Sousa et al., 2009).

Table 1.2.3.1 - Comparison of main applications of different published chromatographic techniques to purify pDNA.

	Chromatographic support	Application	Reference
Gel Filtration	- Superose 6 prep grade	- Resolution of high molecular weight nucleic acids (gDNA and pDNA) from smaller molecules	- Ferreira <i>et al.</i> 1997
	- Sepharacyl S1000 SF	- Reduction of the contaminants of pDNA with gDNA and RNA, using high salt concentration	- Li <i>et al.</i> 2007
Ion Exchange	- Q-Sepharose Big Beads	- Separation of pDNA from gDNA and RNA, with a prior clarification of the sample	- Ferreira <i>et al.</i> 1999
	- Q-Sepharose	- Isolation of sc plasmid from low molecular weight RNA, gDNA and other plasmid forms	- Prazeres <i>et al.</i> 1998
	- Fractogel DEAE	- pDNA purification without RNase application, using prior precipitation and TFF	- Eon-Duval and Bruke 2004
HIC	- Non-porous packing (TSKgel Butyl-NPR)	- Separation of oc and sc pDNA isoforms	- Iuliano <i>et al.</i> 2002
	- Sepharose-gel derivatized with 1,4-butanediol-diglycidylether Biporous support Phenyl-based matrix	- Separation of pDNA from gDNA, RNA, proteins	- Diogo <i>et al.</i> 2000; 2001a; 2001b - Li <i>et al.</i> 2000
	- Superporous crosslinked cellulose - HIC CELBEADS	- Separation of pDNA from RNA and proteins - Separation of pDNA from gDNA, RNA, proteins	- Deshmukh and Lali 2005
Affinity	- IMAC matrices	- Isolation of pDNA and gDNA from RNA, endotoxins and plasmid denatured forms	- Murphy <i>et al.</i> 2003b; Cano <i>et al.</i> 2005; Tan <i>et al.</i> 2007
	- THAC matrices	- Isolation of pDNA; Reduction of RNA and gDNA contamination	- Wils <i>et al.</i> 1997; Schluep and Cooney 1998
	- Protein-based matrices	- Isolation of pDNA; Elimination of RNA and proteins	- Woodgate <i>et al.</i> 2002; Darby <i>et al.</i> 2007
	- Amino acid-based matrices	- Purification of sc pDNA from clarified <i>E. coli</i> lysates	- Sousa <i>et al.</i> 2005; 2006; 2008a; 2009c
(Sousa et al., 2009)			

Within all these chromatographic techniques, ion exchange chromatography (IEC), specifically anion exchange chromatography, remains the most popular as it allows rapid separations, no solvent requirements, sanitization with sodium hydroxide and wide selection of industrial media (Sousa et al., 2009).

Nevertheless, the mechanism of pDNA separation using IEC is still not completely understood and laboratory scale methods, used at industrial scale have reduced yields. For example, in a real approach, for the vaccination of a population, assuming dosages from one to few milligrams, these methods still have to be optimized, and productivities have to be improved to industrial scale, always bearing in mind the guidelines from the regulatory agencies (Ghanem et al., 2013). Additionally, due to economic reasons and despite being more complex to operate than in linear mode, it is important to run the chromatographic processes in the overloaded mode. Thus, chromatographic methods have to be optimized and a better understanding of the mechanisms underlying non-linear chromatography of biomolecules has considerable practical interest (Korfhagen et al., 2010).

1.3. Ion Exchange Liquid Chromatography

Ion Exchange Chromatography (IEC) principle is based on the electrostatic interactions that happen between biomolecules and chromatographic supports. Different molecules exhibit different degrees of interaction with charged chromatography media according to their overall charge, charge density and surface charge distribution. Thus, in IEC, biomolecules are separated according to the differences in their net surface charge.

An IEC medium consists of a matrix substituted with ionic groups that are negatively (Cation Exchange Chromatography, CEC) or positively (Anion Exchange Chromatography, AEC) charged. The medium is packed into a column to form a *peaked bed*. The first step in a chromatographic procedure is to equilibrate the *bed* with a buffer that has adequate pH and ionic strength to bind the interest biomolecule (opposite charge to the medium) and not bind as many as possible impurities (same charge to the medium). Bound biomolecules are concentrated in the column while biomolecules with the same charge as the medium pass through the column, eluting during or just after the sample application. After all the sample has been loaded (and non-binding biomolecules eluted, UV signal returns to baseline), conditions are altered by changing the buffer, usually increasing the ionic strength (salt concentration), leading to the elution of the bound biomolecules. These biomolecules start to elute as the ionic strength increases because salt ions start to compete with the binding sites of the medium. The first biomolecules being eluted from the column are the ones with the lowest net charge at the selected pH, thereafter, the ones with the higher net charge will be most strongly retained and be eluted last. Thus, controlling the changes in ionic strength, different biomolecules can be eluted differentially in a purified and concentrated form. The final step is the regeneration of the column through a very high ionic strength buffer that removes all the tightly bound biomolecules. Before a next run, the column has to be re-equilibrated using the same initial conditions. **Figure 1.3.1** resumes the IEC principles.

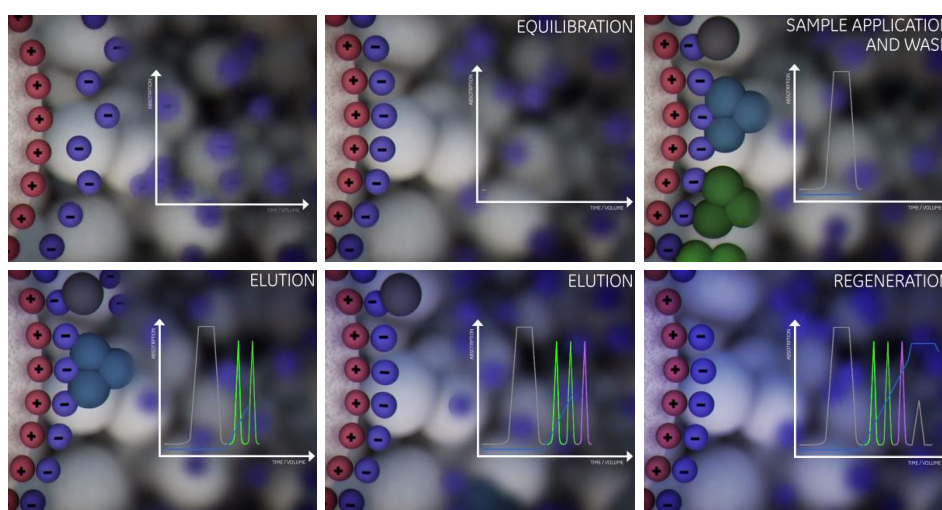


Figure 1.3.1 - Principles of an anion exchange separation (adapted from GE Healthcare)

1.3.1. Anion Exchange Chromatography (AEC) in pDNA purification

Anion exchange chromatography for the purification of pDNA is based on the interaction between the negatively charged phosphate groups on the pDNA backbone and the positively charged groups on the chromatographic medium (stationary phase).

Therapeutic use of pDNA requires not only the removal of host cell contaminants (gDNA, RNA, proteins and endotoxins) but also the purification of sc pDNA from the other less effective isoforms (oc and ln pDNA). Regarding the similarity of the overall charge and molecular weight of the different isoforms, they have different conformations and consequently different local charge densities. Therefore, each isoform will have a different retention time as the elution is promoted by increasing the buffer ionic strength. For instance, sc pDNA has higher charge density than the oc isoform (less constrained), so supercoiled isomer has a stronger interaction and elute later than the oc isoform. However, the interaction of ln pDNA depends not only in the charge density but also in physicochemical properties such as elasticity. Furthermore, other parameters besides charge density, like hydrogen bonding, dispersive forces, dipole-dipole attraction, solvophobic repulsion and Adenine-Thymine (AT) content can influence the adsorption and desorption process.

Anion exchange chromatography major limitation in the purification of pDNA is the non-selectivity of adsorbents leading to the co-elution of impurities, specially endotoxins and high molecular weight RNA (Ghanem et al., 2013).

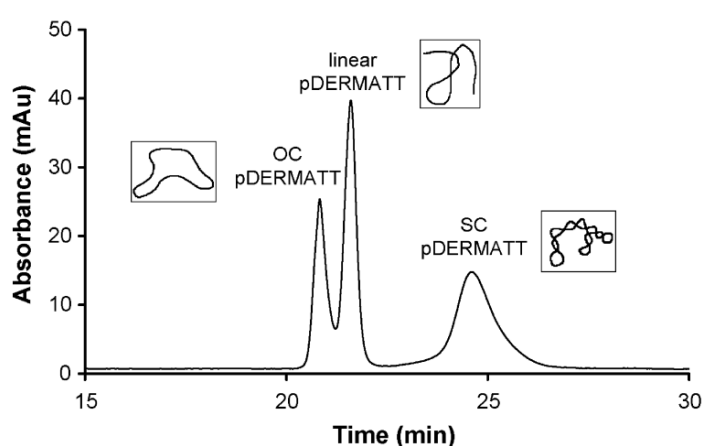


Figure 1.3.1.1 - Representative chromatogram of an anion exchange liquid chromatography separation of linear, circular and supercoiled plasmid (Ghanem et al., 2013)

1.4. Static Binding Capacity

As previously stated, purification yields of industrial scale production of pDNA for pharmaceutical usage have to be improved. This improvement involves the optimization of chromatographic methods, being essential the understanding of the pDNA mechanism of adsorption onto chromatographic supports, considering linear and non-linear conditions.

Generically, adsorption occurs when the adsorbate diffuses from the bulk fluid to the particle surroundings and, in certain cases, through the pores of the particle, where the interaction with the adsorbent takes place, **Figure 1.4.1 (a)**. The molecular mechanisms involved in the adsorption process are film and pore diffusion and interaction kinetics, **Figure 1.4.1 (b)**. To understand the overall adsorption processes is important to study the molecular mechanisms, normally through batch experiments. Parameters estimated in this studies are later used to predict column operations (Ferreira et al., 2000a).

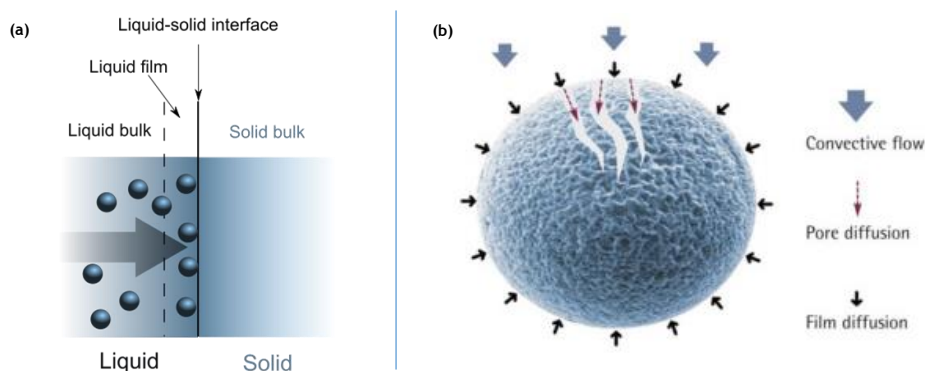


Figure 1.4.1 - (a) Representative adsorption mechanism diagram; (b) Film and pore diffusion (Sartorius Stedim Biotech, 2014)

Protein adsorption have already been explored and several models have been developed to describe adsorption mechanisms and explain equilibrium behaviors (Bellot and Condoret, 1993; Rabe et al., 2011). On the other hand, there still is a lack of data and understanding on the plasmids adsorption mechanism onto chromatographic supports. However it was already suggested that pDNA adsorption onto anion exchangers can be modeled by Langmuir-type isotherms and the surface binding hypotheses have been demonstrated and proposed as the cause for the low capacity of some ion exchange purification methods for pDNA (Ferreira et al., 2000a).

The Langmuir isotherm (Langmuir, 1918) is the simplest theoretical model, that is usually applied to describe biomolecules adsorption. Langmuir isotherm model considers that

adsorption results from a basic reversible interaction between an adsorbate and an adsorbent. Furthermore, it's assumed that the adsorbate molecules have a fixed number of sites on the adsorbent where interactions can occur, and that every adsorption site is energetically equivalent and accepts only one molecule. Additionally, it is considered that there is no interaction between adsorbed molecules (Bellot and Condoret, 1993; Langmuir, 1918).

At low concentrations, biomolecules are well distributed at the adsorbents surface and its orientation is determined by adsorbent-biomolecule interactions, resulting in a linear shaped curve between adsorbed amounts and mobile phase concentration. At high concentrations, the adsorption sites become saturated, leading to a curvature of the isotherm into an asymptote (Bellot and Condoret, 1993; Langmuir, 1918). However, the Langmuir isotherm model may not be applicable to all biomolecules adsorption mechanisms once it does not consider solute-solute interactions neither steric rearrangements on the solute or the support ligands. Despite that, this model still be used as a starting point for the adsorption mechanisms studies (Rabe et al., 2011).

Ferreira *et al* (2000) used Langmuir isotherm model to study pDNA adsorption mechanism in several anion exchangers. A simplistic adsorption-desorption mechanism of a plasmid in an anion exchange process was described by the following equation:



where k_1 and k_{-1} are the adsorption and desorption rate constants, P is the plasmid solution, S represents the adsorption sites and PS the adsorbed plasmid. Thus, the uptake rate of plasmid from the solution is given by:

$$\frac{dQ}{dt} = k_1 C(Q_{\max} - Q) - k_{-1} Q \quad (2)$$

where C is the plasmid concentration in solution, Q is the solid-phase concentration of plasmid, and Q_{\max} is the maximum adsorption capacity of the adsorbent. At equilibrium, the rates of adsorption and desorption are identical and equation (2) can be rearranged:

$$Q = Q_{\max} K_A \frac{C}{1 + K_A C} \quad (3)$$

where $K_A = k_1/k_{-1}$ is the adsorption constant. The solid phase and solution concentrations are considered in equilibrium.

Equation (3) is a Langmuir-type isotherm and if the basic assumption of this model are satisfied, the equilibrium position can be predicted by this equation. **Figure 1.4.2** represents a typical Langmuir isotherm plot.

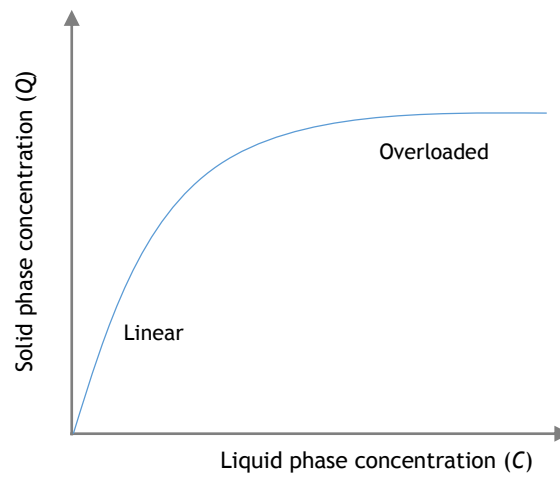


Figure 1.4.2 - Representative Langmuir-type isotherm plot.

1.5. Thermodynamic analysis of biomolecules adsorption

Traditional isotherm models used for ion-exchange adsorption of small molecules are limited once they do not consider non-ideal effects associated with the adsorption of large biomolecules or overloaded conditions, being necessary to include a compensation factor to simulate the equilibrium (Gallant et al., 1995). Despite being a good starting point, traditional models cannot completely characterize complex adsorption mechanisms of biomolecules in liquid chromatography. Whence, these adsorption mechanisms have been elucidated through thermodynamic analysis (Blaschke et al., 2013; Gill et al., 1995; Lin et al., 2001; Silva et al., 2014). Thermodynamic parameters related to adsorption and desorption of biomolecules onto chromatographic media can be accessed performing batch equilibrium experiments, analyzing data through van't Hoff plots or from microcalorimetric measurements (Bellot and Condoret, 1993; Lin et al., 2002; Silva et al., 2014). Batch equilibrium experiments have limited resolution and van't Hoff analysis is an indirect method that becomes too complex in the presence of multiple sub-processes related with adsorption. Furthermore, these methods may not produce representative results of overloaded conditions. Still, calorimetric methods such as Isothermal Titration Microcalorimetry (ITM) and Flow Microcalorimetry (FMC) have shown their aptitude to understand the underlying adsorption mechanism of several biomolecules in several chromatographic media, including linear and non-linear (overloaded) conditions (Blaschke et al., 2013, 2011; Bowen and Pan, 1997; Dieterle et al., 2008; Esquibel-King et al., 1999; Gill et al., 1995; Katiyar et al., 2010; Lin et al., 2001; Pierce et al., 1999; Silva et al., 2014).

1.5.1. Microcalorimetry: Flow (FMC) and Isothermal Titration (ITM)

Biomolecules adsorption and desorption onto chromatographic media are interaction processes between molecules and surfaces. The equilibrium capacity of a surface is dictated by the Gibbs-free energy change for adsorption (ΔG_{ads}), and ΔG_{ads} depends on interaction enthalpy (ΔH_{ads}) and entropy (ΔS_{ads}) (Korfhagen et al., 2010; Lin et al., 2002; Thrash and Pinto, 2002). Biomolecules adsorption and desorption processes have small, but measurable, thermal signals related to their adsorption mechanisms. Thus, through adsorption enthalpy measurements, microcalorimetry can provide valuable understanding of the adsorption mechanisms onto chromatographic media (Bowen and Pan, 1997; Gill et al., 1995; Lin et al., 2002; Silva et al., 2014).

Microcalorimetric methods allow the measurement of the heat flow caused by interaction during the adsorption process of biomolecules onto chromatographic media. In Isothermal Titration Microcalorimetry (ITM) the heat signal is measured in a fed-batch cell as a specific

biomolecule is added to a buffer solution with the adsorbent suspended. Thus, through ITM measurements it's obtained the total energy change in the whole adsorption process, including heat of dilution, interaction heat, the energy required for biomolecule and adsorbent desolvation and dehydration processes and energy change of biomolecule rearrangement after interaction (Lin et al., 2001). Despite providing such information about adsorption, desorption process cannot be accessed by ITM measurements.

Flow Microcalorimetry (FMC) allows a more dynamic measurement of the heat signal as the signal is measured during the adsorption and desorption process of a biomolecule that flows through a small column packed with the adsorbent. As a result, FMC provides an improved understanding of the driving forces, mechanisms and kinetics involved in complete interaction process (Dias-Cabral et al., 2003; Esquibel-King et al., 1999; Katiyar et al., 2010; Ornelas et al., 2013; Raje and Pinto, 1998; Silva et al., 2014; Thrash and Pinto, 2002, 2001; Thrash et al., 2004).

A flow microcalorimeter as the ability to simulate a packed-bed chromatographic system in a micro-scale (**Figure 1.5.1.1**). FMC can be operated under linear or overloaded conditions (Dias-Cabral et al., 2003; Esquibel-King et al., 1999; Silva et al., 2014; Thrash and Pinto, 2002) and results are expected to be representative of the mechanisms that happen in real chromatographic systems. The major advantage of FMC towards a chromatographic system is that the data assessment occurs within the column and not after the column, as in chromatography.

Microcalorimeter test cell (**Figure 1.5.1.1**), where the adsorbent is packed, has a total volume of 171 μL and it's interfaced with two highly sensitive thermistors capable of detecting small temperature changes within the cell (0.1 μWatt) with a thermal response time smaller than 3 s. The system flow rate is controlled by precision syringe micropumps and samples may be injected in the column through a multiport valve system which has a configurable injection loop that can accommodate different sample volumes. After the cell, the effluent passes through an UV detector, allowing to control the biomolecule output. Finally, the effluent can be collected and analyzed by several techniques such as UV spectrophotometry, electrophoresis, circular dichroism, etc.

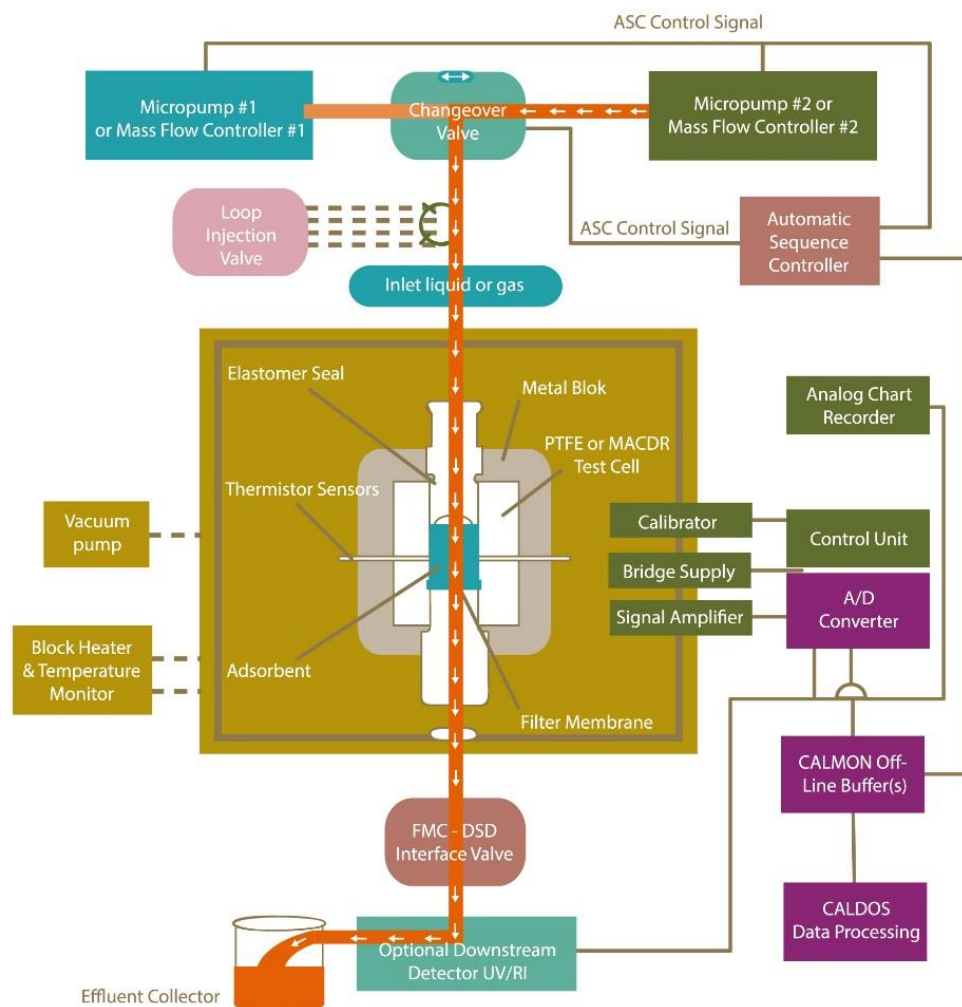


Figure 1.5.1.1 - Representative scheme of the flow microcalorimeter.

Typical FMC thermograms comprise endothermic and exothermic peaks depending on the release or absorption of energy during interactions. Endothermic events (reactions where energy is absorbed) result in negative peaks as the thermistors register a decrease in the cell temperature. On the other hand, exothermic events (reactions where energy is released) result in positive peaks as the thermistors register an increase in the cell temperature. A typical FMC thermogram is represented in **Figure 1.5.1.2**, where the first peak is a calibration peak, with an exothermic profile, that arose from a 30 μW heat impulse during 500 s. Calibration peaks are used to determine the relation between the peaks areas and the its respective energy, also allowing to convert temperature changes assessed by the thermistors in heats of adsorption (Thrash and Pinto, 2002). The second peak in **Figure 1.5.1.2** represents an endothermic event. The third, and last peak, has a skewed shape that represents overlapping events that can be analyzed through the deconvolution of the peak (Phillips and Pinto, 2004).

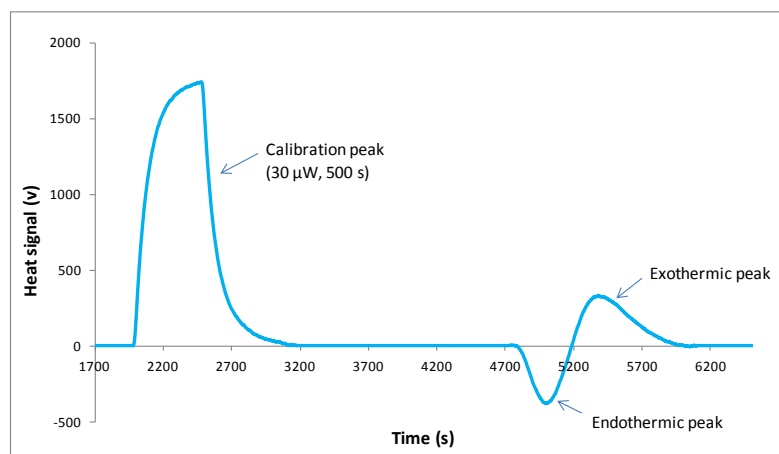


Figure 1.5.1.2 - Typical FMC thermograms for linear pDNA adsorption on Q-Sepharose.

In ion-exchange chromatography, the main interaction between biomolecules and the chromatographic media during adsorption is thought to be the electrostatic interaction, however this is not the only type of interaction during the whole adsorption process. Thermodynamically, previous studies in ion-exchange biomolecules adsorption revealed exothermic events related to electrostatic interaction and endothermic events related to several sources: water and ions release from adsorbent's and biomolecule's surfaces; interaction between protein surface hydrophobic groups and adsorbent hydrophilic moieties; repulsive interactions between same charge groups; biomolecule conformational changes and biomolecule reorientation on the adsorbent surface (Lin et al., 2002; Silva et al., 2014).

Despite the innumerable studies already performed to understand proteins adsorption mechanisms onto several chromatographic systems (Bellot and Condoret, 1993; Blaschke et al., 2013, 2011; Bowen and Pan, 1997; Dias-Cabral et al., 2003; Dieterle et al., 2008; Esquibel-King et al., 1999; Gill et al., 1995; Katiyar et al., 2010; Korfhagen et al., 2010; Lin et al., 2002, 2001; Phillips and Pinto, 2004; Rabe et al., 2011; Raje and Pinto, 1997; Silva et al., 2014; Thrash and Pinto, 2002, 2001; Thrash et al., 2004), there is a lack of data and understanding on the processes of pDNA adsorption onto chromatographic supports (Ferreira et al., 2000a). Ferreira and co-workers (2000), studied the batch adsorption of pDNA onto some anion-exchange chromatographic supports and concluded that is plausible to apply the Langmuir-type isotherms model. However, the data obtained does not account non-ideal effects neither the complexity of working in overloaded conditions.

Phillips and Pinto (2004) performed a study that closely resembles the microcalorimetric adsorption of DNA, investigating the adsorption of nitrogen bases and nucleosides onto a hydrophobic interaction adsorbent. This study revealed that the adsorption behavior of these molecules is a complex phenomenon and although hydrophobic interaction appear to be the primary mechanism for the adsorption, the biomolecules exhibit base stacking behavior. Thus,

the measured heats of adsorption represented the net effect of two different types of interaction: adsorbate/adsorbent interactions and base stacking self-interactions between like molecules (Phillips and Pinto, 2004).

Lastly, Chen and co-workers (2007) performed a study of the interaction mechanism between single-strand (ss) and double-strand (ds) DNA with hydroxyapatite (HA) by Isothermal Titration Microcalorimetry (ITM) and static binding measurements. This study evaluated the effect of different binding parameters such as salt concentration, temperature and pH, and the effect of the ssDNA and dsDNA composition (Guanine-Cytosine (GC) content, length, etc.) on the binding behavior. It was concluded that: due to its higher stability dsDNA has higher binding affinity; an increase in salt concentration decreases dsDNA binding affinity indicating that electrostatic attractions are the main driving force for the interaction; on the other hand, ssDNA binding affinity increases with the increase of the salt concentration once it promotes structural stability and enhances the multilayer formation; temperature decrease promotes structural stability, increasing the ssDNA binding affinity; ITM revealed that the dehydration is the dominant step in the interaction process. In summary, the binding behavior between dsDNA and HA is mainly driven by electrostatic interactions; ssDNA binding is more complex due to the hydrophobic and π - π interaction between bases and the effects of the binding parameters are cross dependent (Chen et al., 2007).

1.6. Goal of Study

As previously mentioned, it is well recognized the importance of plasmid DNA molecules in recent therapies, such as DNA Vaccines and Gene Therapy, for the treatment and cure of several diseases (Ghanem et al., 2013; Ginn et al., 2013; Li et al., 2012; Sousa et al., 2009). The use of pDNA to treat diseases requires its production at the gram scale, with high purity levels and in an economic way, always taking into account the guidelines from the regulatory agencies. Regarding the whole pDNA production, the most challenging step is its purification. Anion-exchange chromatography have been widely and successfully used in pDNA purification (Sousa et al., 2009). Nevertheless, the mechanism of pDNA separation using anion-exchange chromatography is still not completely understood and laboratory scale methods, used at industrial scale, have reduced yields. Additionally, due to economic reasons, it might be important to run the chromatographic processes in the overloaded mode. However, operation in the overloaded mode is considerably more complex than linear chromatography, and suitable models do not exist. Consequently, the prediction of separation behavior is generally unreliable. This is a major impediment in the design and implementation of scaled-up units. Therefore, chromatographic methods have to be optimized and a better understanding of the mechanisms underlying non-linear chromatography of biomolecules has considerable practical interest (Korfhagen et al., 2010). Flow Microcalorimetry (FMC) has proven its ability to provide an improved understanding of the driving forces, mechanisms and kinetics involved in the interaction process on biomolecules adsorption onto several chromatographic systems (Dias-Cabral et al., 2003; Esquibel-King et al., 1999; Katiyar et al., 2010; Ornelas et al., 2013; Raje and Pinto, 1998; Silva et al., 2014; Thrash and Pinto, 2002, 2001; Thrash et al., 2004). Thus, using Flow Microcalorimetry as a central technique, this study aims to understand the interaction between pDNA and anion-exchange supports, considering linear and overloaded conditions and showing the role of nonspecific effects at the adsorptive process. Furthermore, static binding capacity, isothermal titration microcalorimetry and fast performance chromatography will be accomplished to obtain a better understanding of the adsorption mechanism.

2. Material and Methods

2.1. Materials

E. coli DH5 α strain containing 6.05 kbp plasmid pVAX1-lacZ (Invitrogen, Carlsband, CA, USA), **Figure 2.1.1.**, bearing kanamycin resistance gene was obtained from CICS - Health Sciences Research Centre, University of Beira Interior (Covilhã, Portugal)(Sousa et al., 2009). Q-sepharose Fast Flow anion exchanger was obtained from GE Healthcare (Uppsala, Sweden). QIAGEN Plasmid Maxi Kit was obtained from Qiagen (Hilden, Germany). Hind III restriction enzyme was obtained from NZYTech (Lisbon, Portugal). All used reagents were of analytical grade, Sigma-Aldrich (St. Louis, MO, USA).

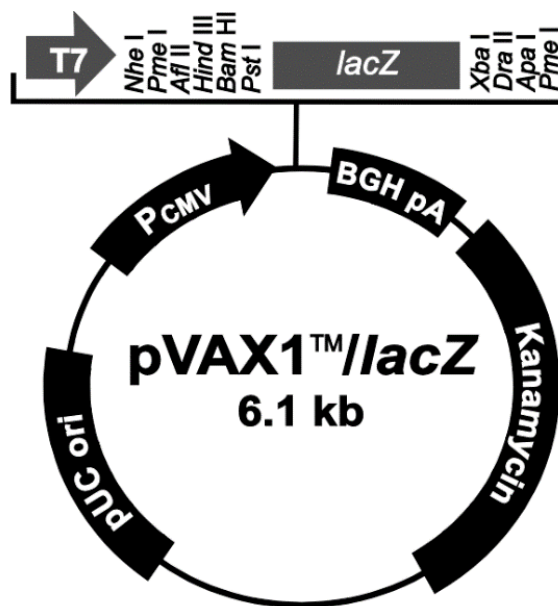


Figure 2.1.1 - pVAX1-LacZ plasmid map from Invitrogen (lifetechnologies.com)

2.2. Apparatus and software

Thermodynamic studies were performed using a Flow Microcalorimeter from Microscal Ltd (London, UK). Data was collected and analyzed in CALDOS4 software from Microscal Ltd (London, UK). Further analysis was done through peak deconvolution using PEAKFIT software package (version 4.12, Seasolve Software Inc., San Jose, USA).

Retention chromatographic data was obtained in ÄKTA Purifier system from GE Healthcare (Uppsala, Sweden). Data was collected and analyzed by UNICORN 5.11 software from GE Healthcare (Uppsala, Sweden).

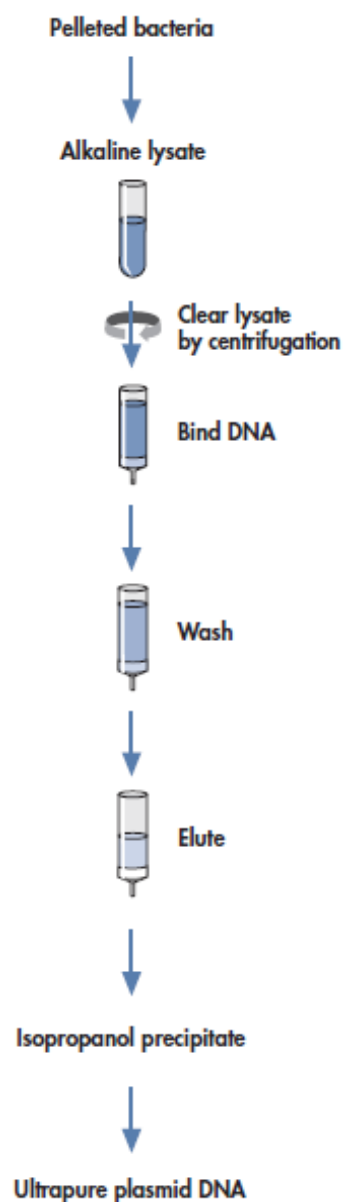
2.3. Plasmid DNA production

2.3.1. Fermentation

E. coli DH5 α cells containing pVAX1-lacZ plasmid were cultivated overnight on solid agar LB medium (Conda Laboratories, Spain) containing 30 μ g/mL of kanamycin antibiotic. Cell colonies grown on the solid medium were collected and inoculated on liquid Terrific Broth (TB) medium (12 g/L tryptone, 24 g/L yeast, 4 mL/L glycerol, 0.017 M KH₂PO₄, 0.072 M K₂HPO₄) supplemented with 30 μ g/mL of kanamycin, for pre-fermentation. That occurred in 500 mL erlenmeyers, containing 125 mL of medium, incubated in an orbital shaker at 37 °C, 250 rpm, until OD₆₀₀ \approx 2.5 was reached. For the fermentation, a fresh batch of liquid TB medium (250 mL in a 1000 mL erlenmeyer) was inoculated from the pre-ferment in order to obtain OD₆₀₀ = 0.2. Fermentation was carried out at 37 °C and 250 rpm, until OD₆₀₀ \geq 6 was reached. After fermentation, cells were recovered by centrifugation (8 min at 5445 g, 4 °C) and the pellets were stored at -20 °C.

2.3.2. Recovery and Purification

Plasmids (pVAX1-LacZ) were recovered from cells using QIAGEN® Plasmid Maxi Kit according to the manufacturer's instructions which are resumed in **Figure 2.3.2.1**.



Alkaline Lysis:

- Bacterial pellet (250 mL of cells) was resuspended in 20 mL of 50 mM Tris-HCl, 10 mM EDTA, 100 µg/mL RNase A, pH 8.0
- Cell lysis was performed by adding 10 mL of 200 mM NaOH, 1% SDS (w/v)
- After 5 min of incubation at room temperature, add 10 mL of prechilled 3 M potassium acetate, pH 5.5 to precipitate genomic DNA, proteins, and cell debris
- Centrifuge twice at ≥ 20000 g for 30 min at 4 °C, reserving the supernatant which contains pDNA

Binding pDNA:

- Equilibrate the QIAGEN-tip by applying 10 mL of 750 mM NaCl, 50 mM MOPS pH 7.0, 15% isopropanol (v/v), 0.15% Triton X-100 (v/v)
- Apply the supernatant from alkaline lysis, allowing the pDNA to connect to the support

Wash:

- Wash the QIAGEN-tip by applying 60 mL of 1 M NaCl, 50 mM MOPS pH 7.0, 15% isopropanol (v/v), permitting the removal of the contaminants that remained in the support

Elute:

- Elute the pDNA by applying 15 mL of 1.25 M NaCl, 50 mM Tris-HCl pH 8.5, 15% isopropanol (v/v)

Precipitate:

- Precipitate the pDNA by adding 0.7 volumes of isopropanol to the eluted pDNA
 - Centrifuge at ≥ 15000 g for 30 min at 4 °C and recover the pellet
 - Redissolve the pDNA pellet in a suitable volume of buffer (e.g. 1 mL of 10 mM Tris-HCl, pH 8.0)
-

Figure 2.3.2.1 - Recovery and purification of pDNA using QIAGEN® Plasmid Maxi Kit.

2.3.3. Agarose Gel Electrophoresis

Isolated pDNA was analyzed by horizontal electrophoresis (110 V, 35 min) using 1% agarose gel in TAE buffer (40 mM Tris, 20 mM Acetic Acid, 1 mM EDTA, pH 8.0) and 0.5 µg/mL of GreenSafe as a nucleic acid stain. Gels were pictured in UVITEC Cambridge system (UVITEC Limited, Cambridge, UK).

2.3.4. Plasmid DNA digestion

In order to ease the pDNA digestion process, samples were previously left overnight at ambient temperature to allow sc pDNA to convert into oc conformation. Then, pDNA linear conformation was obtained by cutting the oc pDNA with restriction endonuclease Hind III according to manufacturer's instructions (incubation at 37 °C during approximately 2 hours adding the adequate buffers). Hind III enzyme was removed from pDNA samples after the digestion through centrifugation, using 100 kDa membrane concentrators (1400 g at 4 °C). For storage and as a carrier fluid the buffer used was 10 mM Tris-HCl, pH 8.0.

2.3.5. Plasmid DNA quantification

Linear plasmid DNA (ln pDNA) concentrations was assessed by absorbance measurement (UV, 260 nm) spectrophotometer (Amersham Biosciences, Uppsala, Sweden). All measurements were performed in triplicates.

2.4. Adsorption Isotherms

Adsorption isotherms were performed in multiwell plates, where 10 mg of dry Q-sepharose have been placed in each well, adding 1 mL of a known concentration of linear plasmid DNA (ln pDNA) in 10 mM Tris-HCl, pH 8.0. The plates were sealed with parafilm and left in the orbital shaker at 230 rpm and 21.5 °C during more than 24 h allowing the equilibrium to be reached (Ferreira et al., 2000a). Thereafter, the slurry was transferred to eppendorf tubes where they were allowed to stand for 30 min. The supernatant was then removed with a syringe, filtered with 0.22 µm membrane filters, and the final concentration of each equilibrium solution was assessed by absorbance measurements (UV, 260 nm) performed in triplicates. To know the

amount of ln pDNA bound to the adsorbent a mass balance was calculated by subtracting the liquid phase concentration to the initial concentration. For the data analysis adsorbed concentration ($\mu\text{g pDNA/g gel}$) was plotted against the liquid phase concentration ($\mu\text{g pDNA/mL}$). Additionally, it were performed control experiments excluding the possibility of pDNA adsorption onto the container walls, where a sample of pDNA with a determined concentration was placed in a well without adding Q-sepharose. Moreover, it was also confirmed that no Q-sepharose particles were released and detected at 280 nm, performing an experiment in a well with Q-sepharose and Tris buffer where no pDNA was added.

2.5. Flow Microcalorimetry (FMC)

Thermodynamic studies were performed in the Flow Microcalorimeter (FMC). FMC column was packed with approximately 21.89 mg of dried Fast Flow Q-sepharose, which after the swelling process filled the 171 μL of the FMC cell. The swelling process was conducted by passing the equilibration buffer through the cell at a constant flow rate of 1.5 mL/h for at least 12 h. The equilibration buffer was 10 mM Tris-HCl (pH 8.0).

Calibration curve was constructed measuring the heat of 5 different energy impulses generated by a specific outlet (calibrator) in the packed cell: 0.3 mJ (3 μW for 100 s), 1 mJ (10 μW for 100 s), 3 mJ (30 μW for 100 s), 7.5 mJ (30 μW for 250 s) and 15 mJ (30 μW for 500 s). All the measurements were performed in triplicates. Considering this range of energy, the relation between the energy impulse and the resulting heat (peak area) was linear. These experiments also allow to determine the calibration factor of the packed system. This factor will be later used to convert cell temperature changes in heat signals.

To study the adsorption of ln pDNA (pVAX1-LacZ) onto Fast Flow Q-sepharose, first the system was packed as explained above and, after the thermal equilibrium was reached, a sample of ln pDNA prepared in 10 mM Tris pH 8.0 was loaded into a configurable injection loop (of 30, 229, 429 or 1000 μL) and then injected into the cell through switching a multiport valve, using a constant flow rate of 1.5 mL/h. The adsorption process of the sample into the adsorbent surface causes a temperature change in the cell, which through the calibration factor is converted to a heat signal by the FMC. CALDOS 4 software was used to acquire, store, process and present all the FMC data. In order to know the adsorbed quantity of ln pDNA a mass balance was calculated subtracting the concentration of the collected effluent to the concentration of the injected sample. Those concentrations were assessed by measuring the 260 nm absorbance in the UV spectrophotometer. Between injections, it was used 1 M NaOH as a washing solution and the system was re-equilibrated with 10 mM Tris pH 8.0 (G.E. Healthcare, 2007).

2.6. Isothermal Titration Microcalorimetry (ITM)

Isothermal Titration Microcalorimetry (ITM) experiments were also performed in the Flow Microcalorimeter using its static mode of operation. Microcalorimeter column was packed with approximately 3.5 mg of dried Fast Flow Q-sepharose, which were suspended in 100 μ L of 10 mM Tris pH 8.0. The system thermal equilibrium was reached 3h after packing, then an automatic pattern was used to perform the experiments in which a ln pDNA sample of 30 μ L was titrated into the cell using a pump controlled syringe. Experiments where the pDNA sample or the adsorbent or both were absent were also performed to be used as blank experiments. Data was acquired, stored and processed by CALDOS4 software.

2.7. Fast performance chromatography

A XK empty chromatographic column (GE Healthcare, Uppsala, Sweden) was packed with Fast Flow Q-sepharose and experiments were performed in ÄKTA Purifier system. Before each retention measurement, the system was equilibrated with at least 5 column volumes of working buffer, 10 mM Tris pH 8.0 supplemented with 2, 1, 0.8, 0.7, 0.6 or 0.5 M of NaCl, at a constant flow rate of 1 mL/min. After equilibrating the column with the working buffer, a 20 μ L ln pDNA sample (prepared in the same buffer conditions) was injected and the retention time was measured. Between each retention time measurement, the column was cleaned using the washing buffer 2 M NaCl, 10 mM Tris pH 8.0 to remove the retained molecules, then equilibrated with 10 mM Tris pH 8.0, and finally equilibrated with the next working buffer. Retention times and other chromatographic data was collected and analyzed by UNICORN 5.11 software.

3. Results and Discussion

3.1. Plasmid DNA production

After each *E. coli* DH5 α fermentation it was obtained about 250 mL of cells. The use of the Qiagen Plasmid Maxi kit[®] yielded approximately a final concentration of 600 $\mu\text{g/mL}$ of 6.05 kbp pVAX1-lacZ plasmid DNA (ln, oc and sc isoforms, **Figure 3.1.1 [A]**). Subsequently, the pDNA was left at room temperature and, as time passed, it was noticed an increase in the relative amount of open circular and linear pDNA and a parallel decrease in the relative amount of supercoiled DNA. In the 3rd day there was only open circular and linear pDNA, **Figure 3.1.1 [D]-(a)**, after that the samples were digested with the restriction enzyme Hind III to obtain only linear pDNA, **Figure 3.1.1 [D]-(b)**.

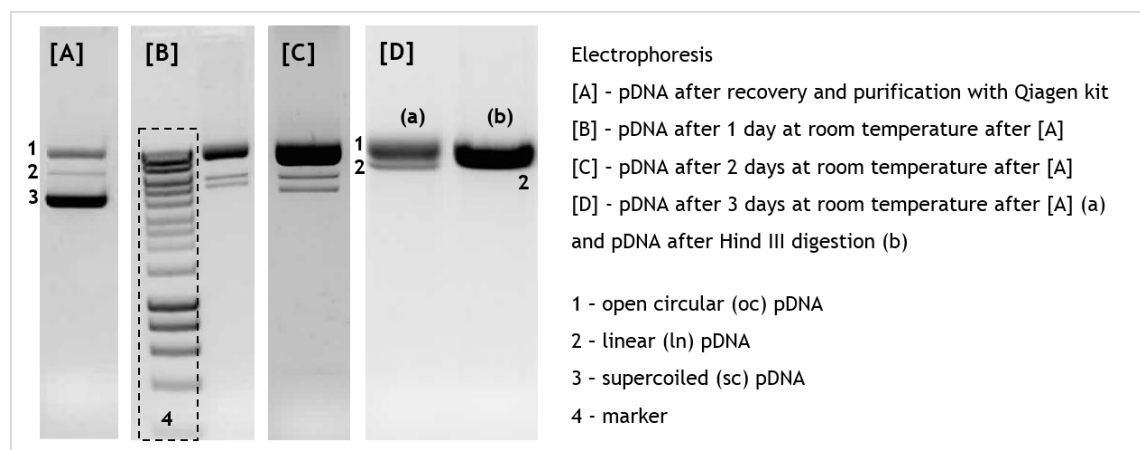


Figure 3.1.1 - Electrophoresis resumed results.

3.2. Static Binding Capacity

Static binding capacity studies of linear pDNA (pVAX1-LacZ) adsorption onto Fast Flow Q-sepharose are reported by the following equilibrium binding isotherm, **Figure 3.2.1**. Through the analysis of the isotherm profile, it can be seen that the adsorption capacity (q_{pDNA}) increases from zero to a plateau region as the ln pDNA equilibrium liquid concentration (C_{pDNA}) increases. Within the range covered in this study, the shape of the curve fits to the Langmuir-type isotherm profile (Bellot and Condoret, 1993; Langmuir, 1918).

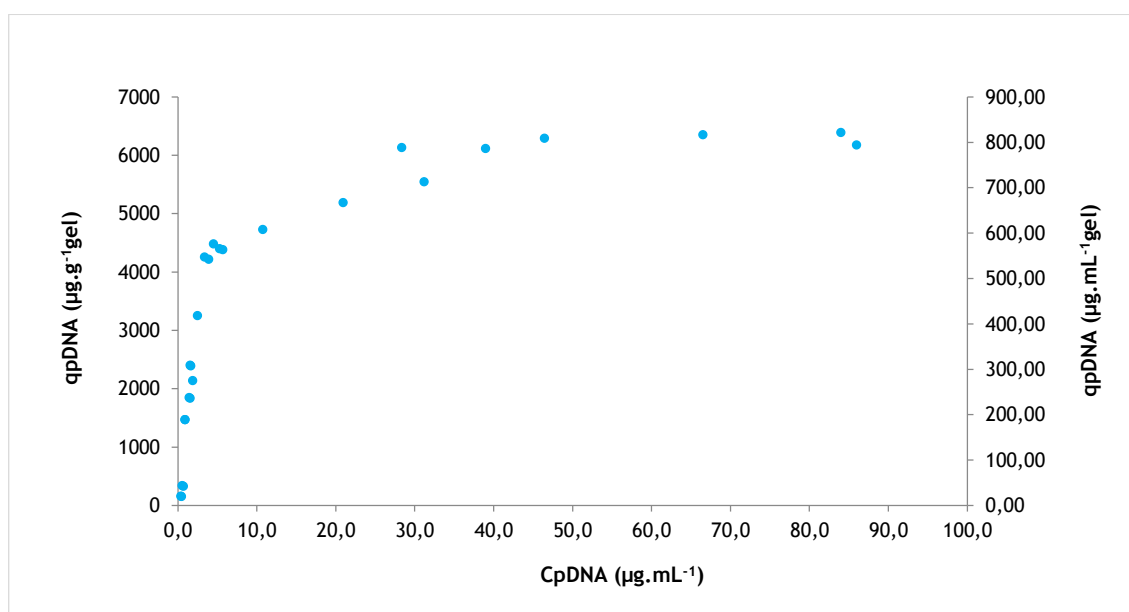


Figure 3.2.1 - Equilibrium binding isotherm for ln pDNA (pVAX1-LacZ) adsorption onto Fast Flow Q-sepharose using 10 mM Tris, pH 8.0 at 21.5°C.

Ferreira and co-workers (2000), studied the batch adsorption of a 4.8 kbp pDNA (pMa5-L) onto some anion-exchange chromatographic supports (Q-Sepharose High Performance, Fast Flow, Big Beads and Streamline QXL) adding different salt concentrations to the equilibrium buffer (0.5, 0.7 and 1 M NaCl). No plasmid adsorption was observed at 1 M NaCl and data from 0.5 and 0.7 M NaCl were fitted with Langmuir-type isotherms, even though the effect of the co- and counterion is not taken into account by this isotherm model. Furthermore, it was observed that the maximum binding capacities were independent of the ionic strength in the tested range (Ferreira et al., 2000a). Our fast performance chromatography experiments revealed that there is no variation of the retention time using different ionic strength conditions, for the interaction between the pDNA and the FF Q-sepharose. In 2, 1 and 0.8 M NaCl experiments it was observed a retention time of 1.30 min, coincident with the retention time of a non-retained component. Remaining salt concentrations (0.7, 0.6 and 0.5 M NaCl) resulted in a total retention of the ln pDNA in the column. Bearing in mind the relation between the retention factor (k') and the

equilibrium binding constant (K), $k' = K \times \Phi$ (Lin et al., 2002), and once the phase ratio of the column (Φ) is constant, one can say that the retention factor and the equilibrium binding constant are directly proportional. However, since we couldn't see the influence of salt concentration on the pDNA retention behavior, no conclusions can be drawn. Nevertheless, despite our study used a different plasmid and was performed in absence of salt, comparing with Prazeres and co-workers (Ferreira et al., 2000a), obtained equilibrium isotherms for pDNA adsorption onto FF Q-sepharose have the same shape and similar adsorption capacities.

Considering the equilibrium binding isotherm data, **Figure 3.2.2**, it is possible to define a linear and an overloaded zone. Values of pDNA adsorbed concentration (q_{pDNA}) above 4000 $\mu\text{g}\cdot\text{g}^{-1}\text{gel}$ are considered in the overloaded zone of the isotherm. Moreover, according to the equilibrium binding isotherm shape, within the range studied, it's not expected the occurrence of multilayer adsorption, once when this phenomenon occurs, a second increase in the adsorbed concentration is observed after the first plateau in the isotherm (Chen et al., 2007).

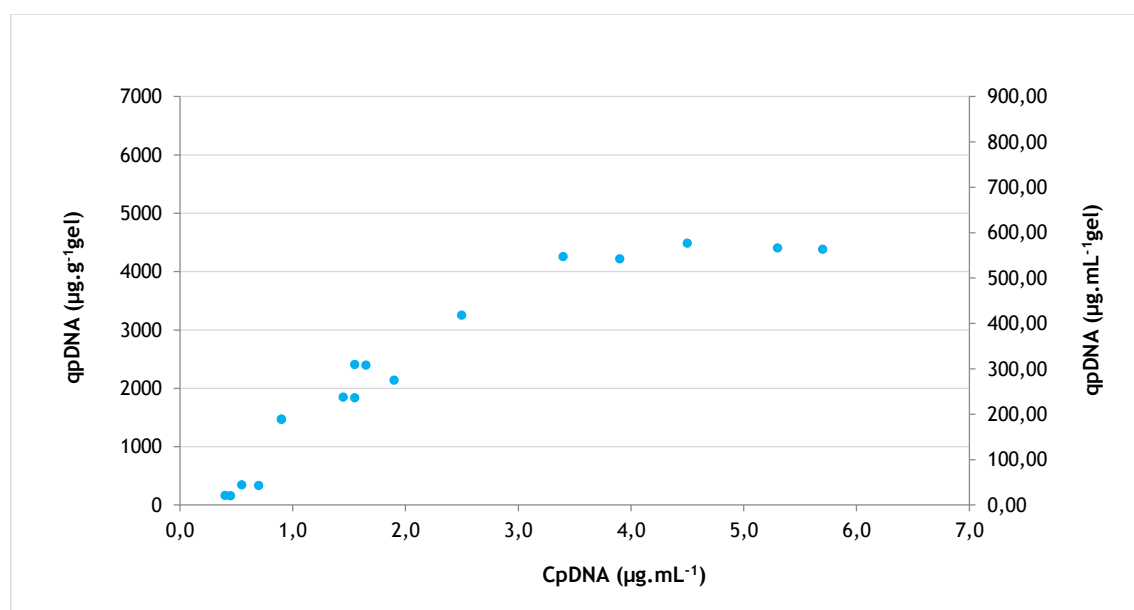


Figure 3.2.2 - “Zoom-in” of the low equilibrium concentration zone of isotherm from Figure 3.2.1.

3.3. Flow Microcalorimetry (FMC)

Flow Microcalorimetry (FMC) experiments were performed to understand the interaction between pDNA (pVAX1-LacZ) and the anion-exchange support Fast Flow Q-sepharose, considering linear and overloaded conditions and to show the role of nonspecific effects at the adsorptive process. Through the knowledge of the magnitude and chronology of thermal events during and after the biomolecule-adsorbent interaction, the adsorption mechanism can be elucidated (Dias-Cabral et al., 2003; Katiyar et al., 2010; Kim et al., 2013, 2011a, 2011b; Thrash and Pinto, 2002, 2001; Thrash et al., 2004).

Experiments were performed using different injection loops (30, 229, 429 and 1000 μL). The pDNA injection concentrations varied from 5.40 to 475.00 $\mu\text{g}/\text{mL}$ for the 30 μL loop, from 59.00 to 475.00 $\mu\text{g}/\text{mL}$ for the 229 μL loop, from 100.42 to 518.00 $\mu\text{g}/\text{mL}$ for the 429 μL loop and from 111.17 $\mu\text{g}/\text{mL}$ to 188.50 for the 1000 μL loop, resulting in different loadings of pDNA (Table 3.3.1).

Table 3.3.1 - Feed and loading concentrations for ln pDNA adsorption onto FF Q-sepharose using different loops.

Loop (μL)	30			229			429			1000	
[pDNA] feed ($\mu\text{g}/\text{mL}$)	9.25	39.40	82.00	59.00	90.30	138.50	135.00	204.50	475.00	111.17	180.50
pDNA mass feed (μg)	0.27	1.17	2.43	13.51	20.68	31.72	57.92	87.73	203.78	111.17	188.50
pDNA loading ($\mu\text{g}/\text{g}$)	12.55	53.35	111.23	576.58	820.41	1222.50	1359.63	3599.01	5489.43	1830.54	3884.83

Figures 3.3.1 - 3.3.4 illustrate some examples of the thermograms obtained with the different injection loops. In each graphic different signals resulted from different loading concentrations, obtained in the same (linear) or in different zones of the isotherm (linear, transition and overloaded). All thermograms comprised a first endothermic peak followed by an exothermic one which may result from the overlapping of different peaks.

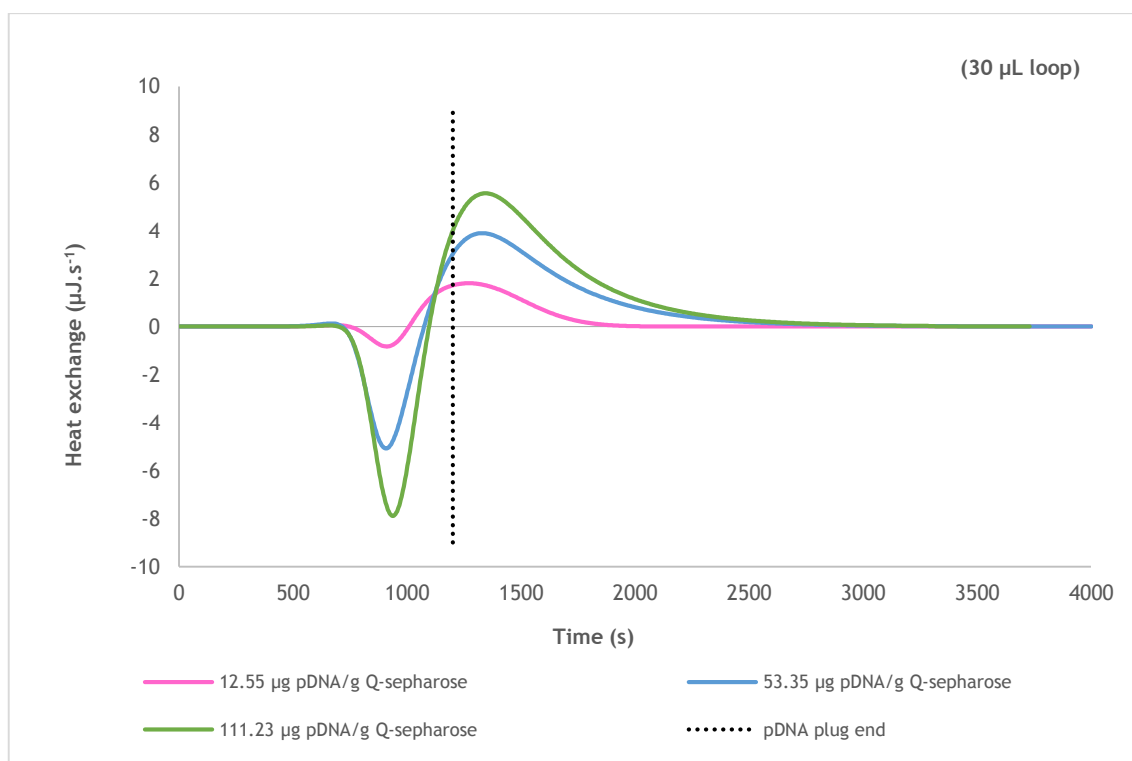


Figure 3.3.1 - Thermograms of ln pDNA (pVAX1-LacZ) adsorption onto FF Q-sepharose using the 30 μL loop.

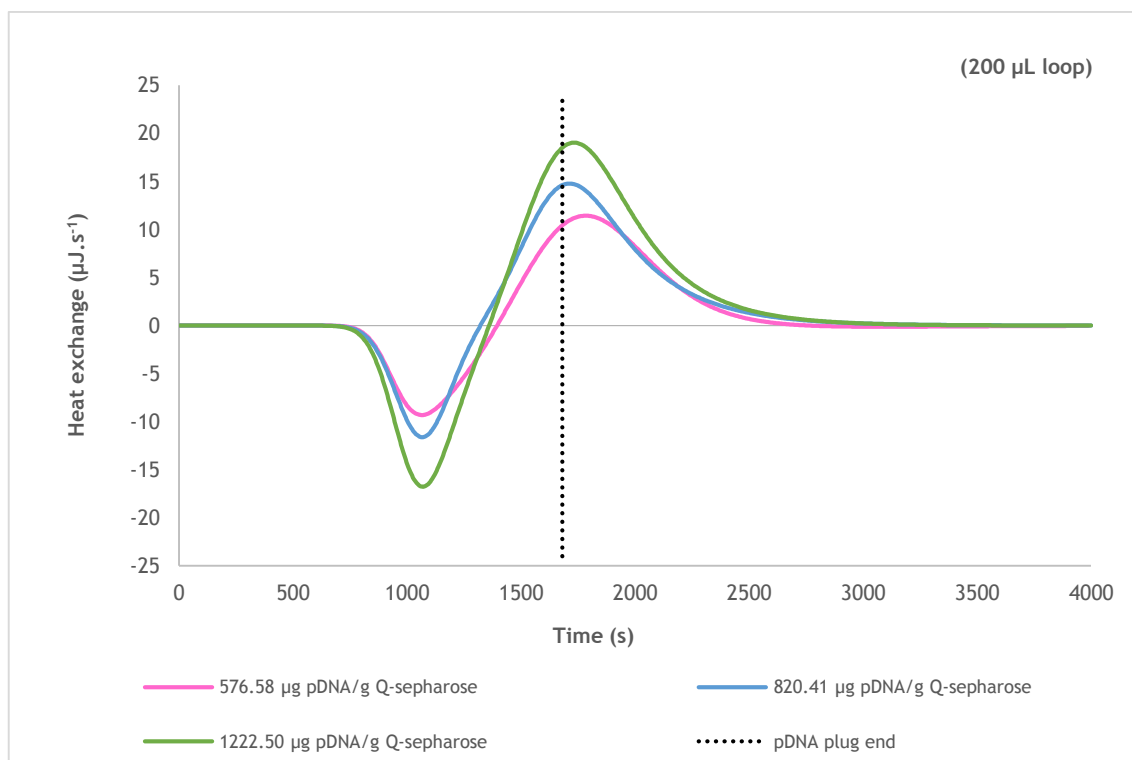


Figure 3.3.2 - Thermograms of ln pDNA (pVAX1-LacZ) adsorption onto FF Q-sepharose using the 229 μL loop.

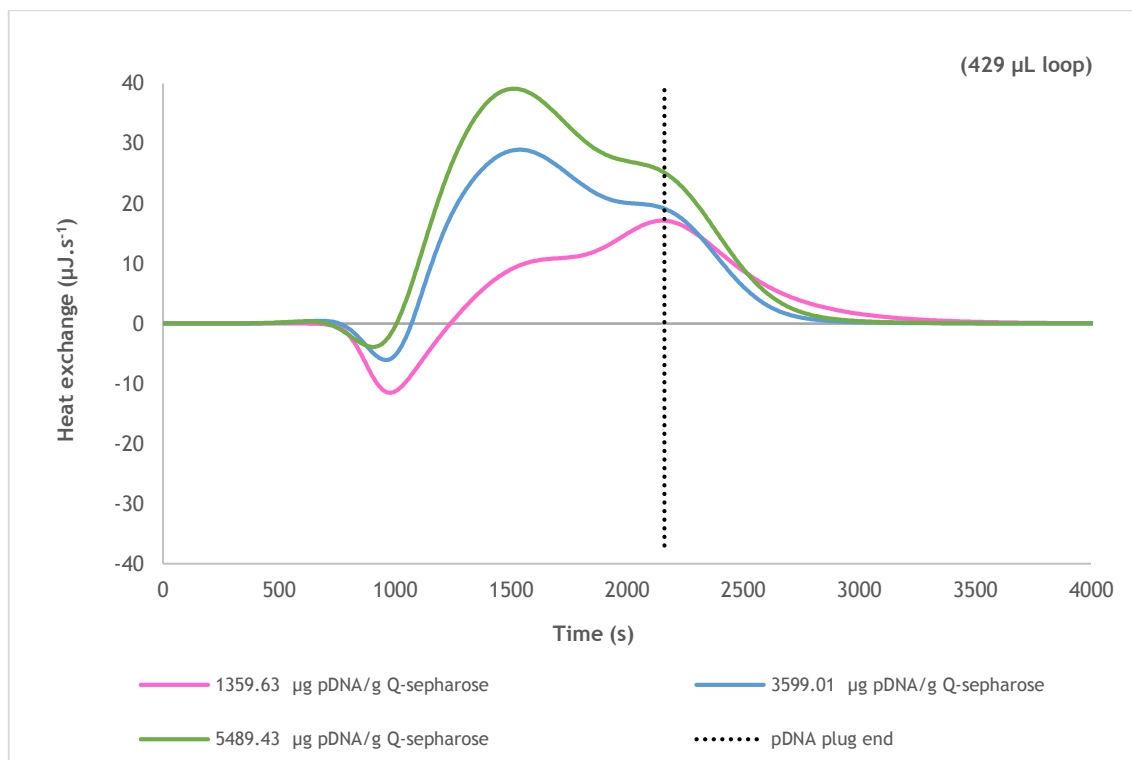


Figure 3.3.3 - Thermograms of ln pDNA (pVAX1-LacZ) adsorption onto FF Q-sepharose using the 429 μL loop.

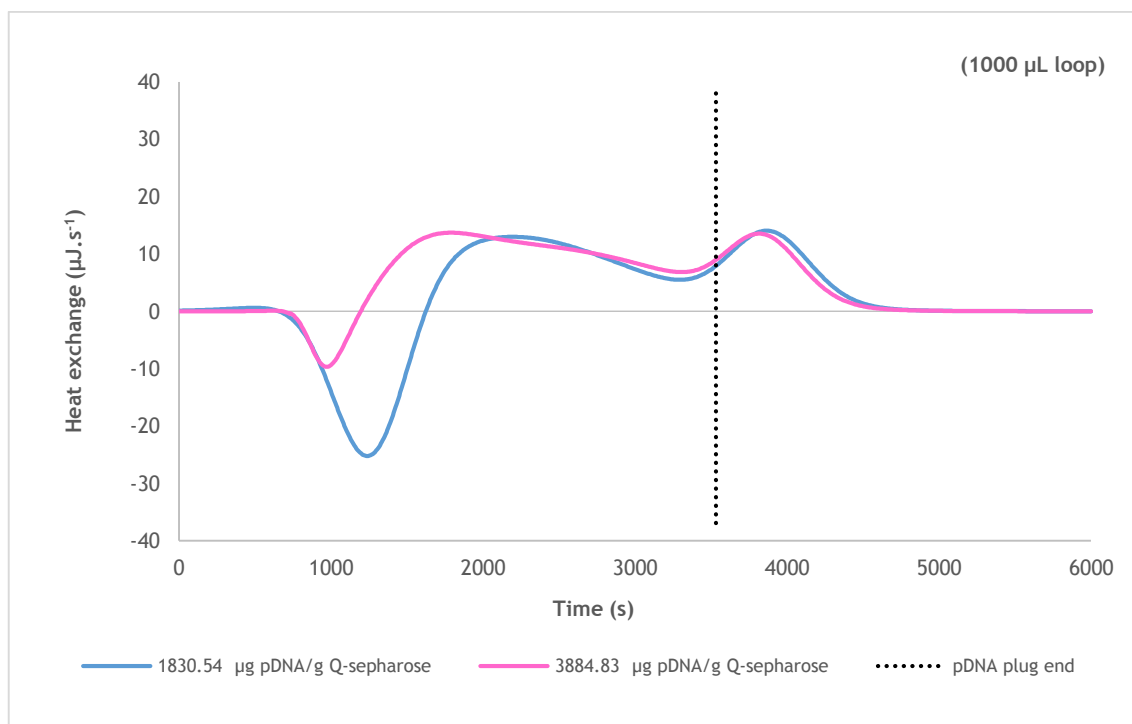


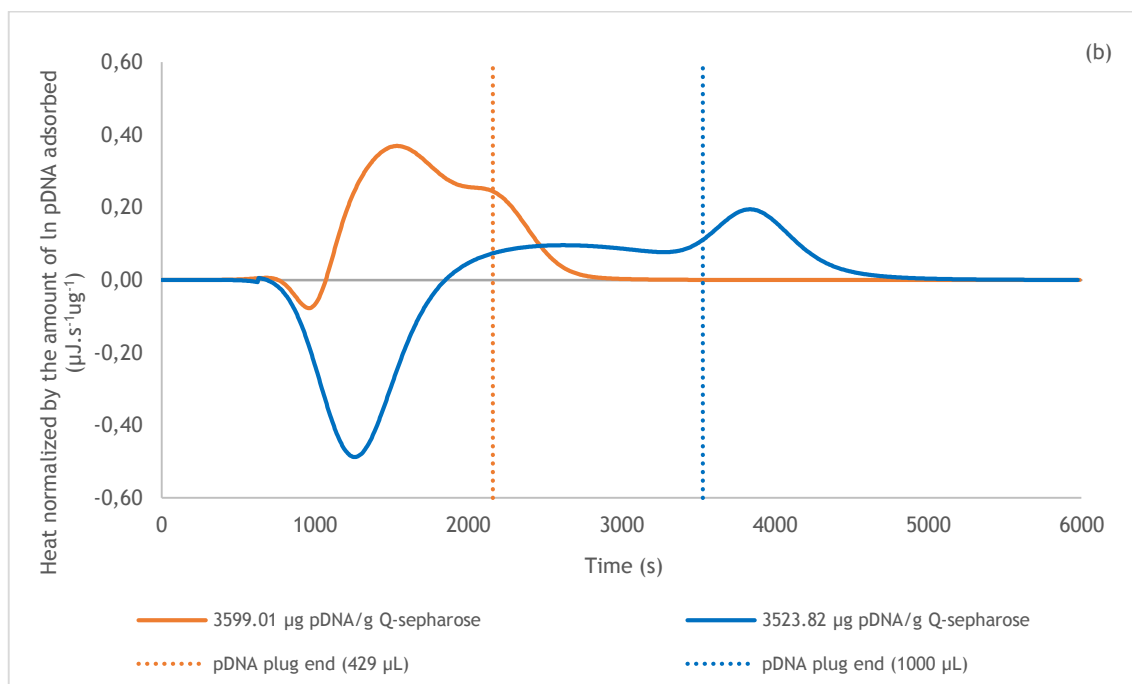
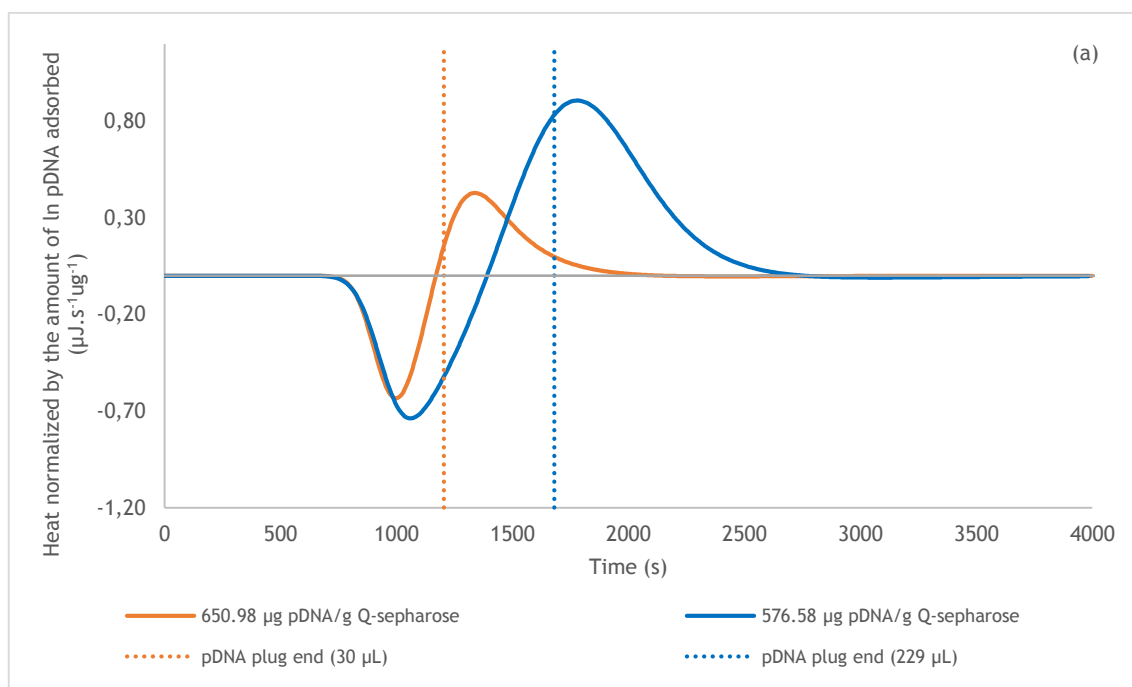
Figure 3.3.4 - Thermograms of ln pDNA (pVAX1-LacZ) adsorption onto FF Q-sepharose using the 1000 μL loop.

Bearing in mind the 171 μL of the FMC cell, the use of the 30 μL loop means that the sample is introduced into the column as a pulse (30 μL represents 0.2 times the cell volume). The use of the 229 μL loop fulfils the FMC cell, representing 1.3 times of the cell volume. On the other hand, the use of the 429 μL and 1000 μL loops represents 2.5 and 5.8 times the cell volume respectively, leading to a continuous feed of the biomolecule into the column, resembling the frontal analysis in chromatographic systems (Carta and Jungbauer, 2010).

Considering the thermograms obtained using the 30 and the 229 μL loops (**Figures 3.3.1 and 3.3.2**) it is observed that the heat signal presents a similar profile and that both the endothermic and the exothermic events increase in magnitude as the pDNA loading concentration increases (initial concentrations). Conversely, comparing the obtained thermograms using the 229 and the 429 μL loops (**Figures 3.3.2 and 3.3.3**), and considering similar loading concentrations (1222.50 $\mu\text{g/g}$ for the 229 μL loop and 1359.63 $\mu\text{g/g}$ for the 429 μL loop) it can be seen a change in the peak profile, length and magnitude. Thus, it is evidenced that the transition from a pulse injection (229 μL loop) to a continuous feed (429 μL loop) leads to alterations in the peak profile. Moreover, by increasing the loop further (from the 429 μL loop to the 1000 μL loop, **Figures 3.3.3 and 3.3.4**) for similar loading concentrations (3599.01 $\mu\text{g/g}$ for the 429 μL loop and 3884.83 $\mu\text{g/g}$ for the 1000 μL loop) the profile of the peak remains similar whereas the time of the whole interaction increases leading to a change in the magnitude of the heat signal and in the time at which each event took place.

In order to allow the direct energetic comparison between the different injection loops, heat signals were normalized by the amount of pDNA adsorbed at equilibrium (**Figure 3.3.5**). It is important to mention that the loading pDNA concentration obtained with the 30 and 229 μL loops were only in the linear zone of the isotherm while, with the 429 and 1000 μL loops results were obtained at loading concentrations at all the isotherm zones (linear, transition and overloaded). **Figures 3.3.5 (a), (b) and (c)** compare similar pDNA loading concentrations thermograms using different loops (a: 30 and 229 μL ; b: 429 and 1000 μL ; c: 229 and 429 μL). It can be better observed and stated once again, that thermograms obtained with 30 and 229 μL (**Figure 3.3.5 a**) have the same signal profile, presenting differences in the heat signal magnitude, in the length of the whole interaction and at the time which each event took place. The same applies for the thermograms obtained with 429 and 1000 μL (**Figure 3.3.5 b**). This phenomenon occurs due to the increase in biomolecule resident time at the system, which gives more time for the equilibrium establishment. Dias-Cabral and co-workers had already detected these phenomena using different pulse injection loop sizes in the FMC (Silva et al., 2014). Finally, due the differences between a pulse and a continuous feed, the signal profile of the thermograms obtained with 229 and 429 μL have different profiles (**Figure 3.3.5 c**). This is to be expected, once in presence of the higher loop we are working in conditions of volume overloading, this will be discussed later.

Accordingly to the exposed, further analysis of the data was performed considering the 30 and the 229 μL loops data separately from the 429 and the 1000 μL loops data.



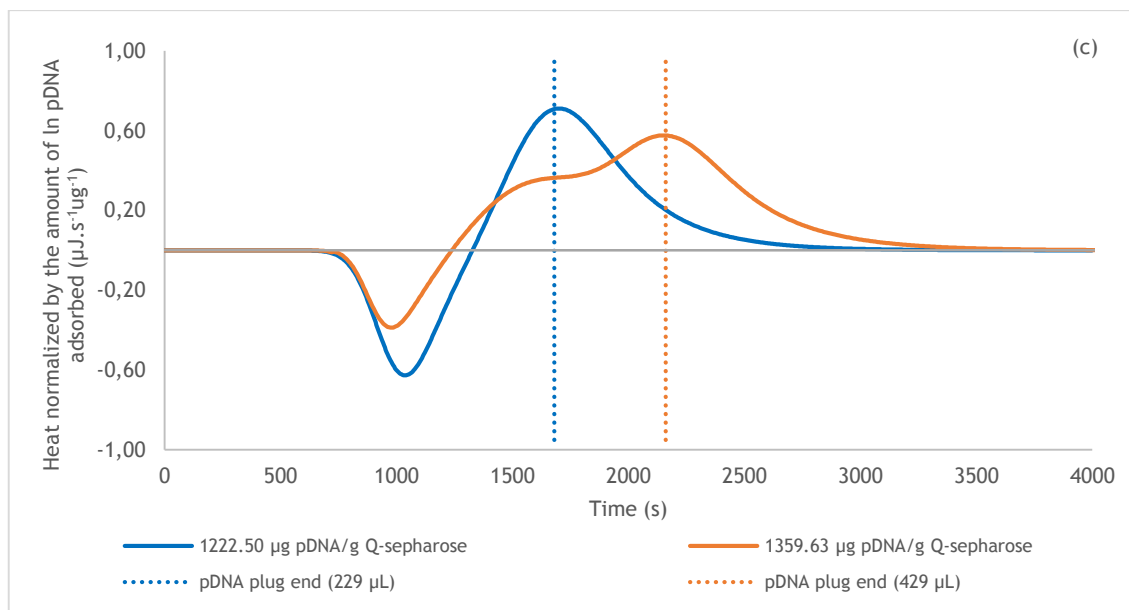


Figure 3.3.5 - Thermograms of ln pDNA (pVAX1-LacZ) adsorption onto FF Q-sepharose, similar loading concentrations using different loops: (a) 30 and 229 μL ; (b) 429 and 1000 μL ; (2) 229 and 429 μL .

The presence of different peaks in a thermogram (**Figures 3.3.1 - 3.3.4**) suggests the existence of different events during the adsorption process. These events may occur in a sequence (one peak after another one) or simultaneously (overlapping peaks). Peak symmetry test (Esquibel-King et al., 1999) revealed the presence of overlapped peaks, thus thermograms were de-convoluted using the PeakFIT software as explained previously in “Materials and Methods”.

Thermograms in **Figure 3.3.6** show the de-convolution of the heat signals obtained by CALDOS 4 for four experiments using the 30 μL loop, in the linear zone of the isotherm. The enthalpy changes determined from the deconvoluted thermograms for each step in the process by which pDNA adsorbs on Q-sepharose are summarized in **Table 3.3.2**.

Table 3.3.2 - Heat of adsorption for ln pDNA adsorption onto FF Q-sepharose (**Figure 3.3.6**).

Loop (μL)	pDNA mass feed (μg)	pDNA loading ($\mu\text{g/g}$)	Endothermic Peak ($\text{mJ}/\mu\text{g}$)	Exothermic Peaks ($\text{mJ}/\mu\text{g}$)			Net heat of adsorption ($\text{mJ}/\mu\text{g}$)
			ΔH^{I}	ΔH^{II}	ΔH^{III}	$\Delta H^{\text{II}} + \Delta H^{\text{III}}$	ΔH^{Total}
30	0.27	12.55	1.160	-3.912	0	-3.912	-2.752
	1.17	53.35	2.164	-3.451	0	-3.451	-1.287
	2.43	111.03	1.642	-2.048	0	-1.839	-0.406
	14.25	650.98	0.364	-0.374	0	-0.374	-0.010

$$\Delta H^{\text{Total}} = \Delta H^{\text{I}} + \Delta H^{\text{II}} + \Delta H^{\text{III}}$$

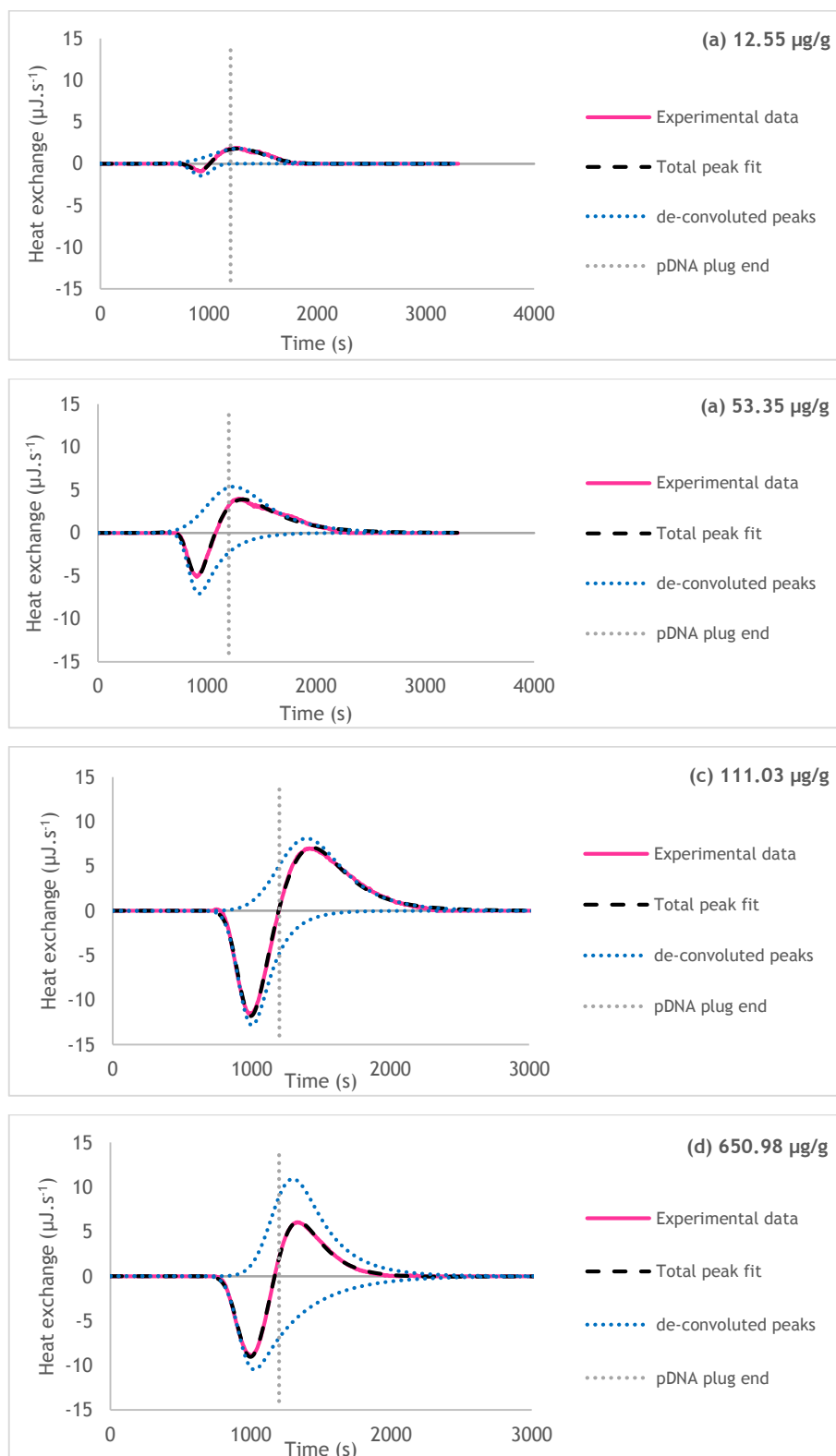


Figure 3.3.6 - PeakFIT de-convolution of thermograms for ln pDNA adsorption onto FF Q-sepharose for different loading concentrations, using the 30 μL loop: (a) 12.55 μg pDNA/g Q-sepharose; (b) 53.35 μg pDNA/g Q-sepharose; (c) 111.03 μg pDNA/g Q-sepharose; (d) 650.98 μg pDNA/g Q-sepharose.

In all studied cases, the first peak emerges at the exact moment when the frontal boundary of the pDNA solution reaches the packed medium in the FMC cell. It can also be seen that the endothermic and exothermic signals overlap.

Previous calorimetric studies of biomolecules adsorption have revealed that endothermic events were related to different sources (according to the process conditions): desolvation process (dehydration and de-counter ion of biomolecule and adsorbent surfaces) (Chen et al., 2007; Korfhagen et al., 2010; Silva et al., 2014); repulsive interaction between hydrophobic and hydrophilic groups and between like charged groups (Katiyar et al., 2010; Lin et al., 2001; Thrash and Pinto, 2002); and, biomolecules conformational changes or surface reorientation, as well as solvation and hydration of bound molecules (Chen et al., 2007). On the other hand, exothermic events occur when attractive forces are present and/or dominant (Chen et al., 2007; Katiyar et al., 2010; Kim et al., 2013, 2011a, 2011b; Korfhagen et al., 2010; Thrash and Pinto, 2002).

To analyze the de-convoluted thermograms, the mechanism proposed by Yamamoto and co-workers (Lin et al., 2001) for the ion exchange adsorption will be considered. They suggest that this adsorption can be divided into five sequential sub-processes: (i) water molecules and ions release from the biomolecule surface; (ii) water molecules and ions release from the adsorbent surface; (iii) electrostatic and/or hydrophobic interactions between the biomolecule and the ion exchanger; (iv) structural conformation rearrangement and reorientation of the adsorbed biomolecules; (v) rearrangement of the excluded water molecules and ions in the solution. Thus, the endothermic heat signal could be related to the sub-process (i), (ii), (iv) and (v), and the exothermic heat signal to the sub-process (iii) (Lin et al., 2001; Silva et al., 2014).

Taking into account the de-convoluted peaks (**Figure 3.3.6**), it is important to refer that at the time when the mobile phase plug containing pDNA was replaced with pDNA-free mobile phase (around 1200 s) either the endothermic and exothermic peaks have not yet returned to the baseline, suggesting the occurrence of simultaneous thermal events. Furthermore, during the time when pDNA is flowing through the column (before 1200 s) the endothermic peak area is larger than the exothermic one. Once in a favorable interaction, the Gibbs free energy has to be negative, here the adsorption process has to be entropically driven. Thus, considering the above assumptions (i-v), during the interaction between the pDNA and the FF Q-sepharose, the desolvation process, including dehydration and release of counter ions from the biomolecules and adsorbent surfaces (i, ii), may be the main role, leading to an endothermic heat of adsorption. That is, the endothermic heat due to desolvation is compensated by the entropy gain resulting from the release of water and ions (Chen et al., 2007; Korfhagen et al., 2010; Thrash et al., 2004). The water molecules quantification would be an interesting proof of this phenomenon, however the fast performance chromatography experiments revealed no difference in the retention times using different ionic strengths, being not possible to perform

the Perkins analysis and calculate the number of water molecules (Perkins et al., 1997). Nevertheless, according to the chronological sequence of sub-processes proposed by Yamamoto and co-workers (2001), the first event is endothermic and compatible with the desolvation process. Besides this, endothermic heats of adsorption were related to the (1) water release due to hydrophobic interactions, (2) solvation and hydration process of the bound pDNA-Q-sepharose, (3) structural rearrangements of pDNA and (4) repulsion between adsorbed biomolecules. However, under the studied conditions hydrophobic interaction appears not to be a major contributor to the observed endothermic heat, since we are working in absence of salt, FF Q-sepharose is considered a strong anion exchanger and at pH greater than 4, DNA appears as a polyanionic molecule (Ferreira, 2005). Also sub-processes (2) and (3) involve heat changes that were considered minimal when compared to heat changes present in desolvation and interaction sub-processes (Chen et al., 2007; Silva et al., 2014). Since we are still working in the linear zone of the isotherm, sub-process (4) is expected to have also a negligible contribution. Thus, desolvation process seems to be the major contributor to the observed endothermic signal.

Simultaneously to the water molecules and ions release in the desolvation sub-process the interaction of ln pDNA and FF Q-sepharose occurs through an electrostatic attraction, leading to the arise of the exothermic peak in the thermogram. The fact that the maximum of the exothermic peak appears after the end of the pDNA plug (after the mobile phase plug containing pDNA was replaced with pDNA-free mobile phase) suggests the presence of other thermal events. These may be due to secondary adsorption of bound pDNA (biomolecules reorientation) which may occur due to the flexibility characteristic of ln pDNA (Smith et al., 2007).

Thermograms in **Figure 3.3.7** show the de-convolution of the heat signals obtained by CALDOS 4 for four experiments using the 429 μL loop, in the linear, transition and overloaded zones of the isotherm. The enthalpy changes determined from the deconvoluted thermograms for each step in the process by which pDNA adsorbs on Q-sepharose are summarized in **Table 3.3.3**. The obtained heat signal is characterized by an endothermic peak followed by two overlapping exothermic peaks.

Table 3.3.3 - Heat of adsorption for ln pDNA adsorption onto FF Q-sepharose using the 429 μL loop.

Loop (μL)	pDNA feed (μg)	pDNA loading ($\mu\text{g/g}$)	Endothermic Peak ($\text{mJ}/\mu\text{g}$)	Exothermic Peaks ($\text{mJ}/\mu\text{g}$)			Net heat of adsorption ($\text{mJ}/\mu\text{g}$)
			ΔH^{I}	ΔH^{II}	ΔH^{III}	$\Delta H^{\text{II}} + \Delta H^{\text{III}}$	ΔH^{Total}
429	57.92	1359.63	0.189	-0.293	-0.363	-0.656	-0.467
	87.73	3599.01	0.045	-0.321	-0.082	-0.403	-0.358
	203.78	5489.43	0.033	-0.287	-0.077	-0.364	-0.331

$$\Delta H^{\text{Total}} = \Delta H^{\text{I}} + \Delta H^{\text{II}} + \Delta H^{\text{III}}$$

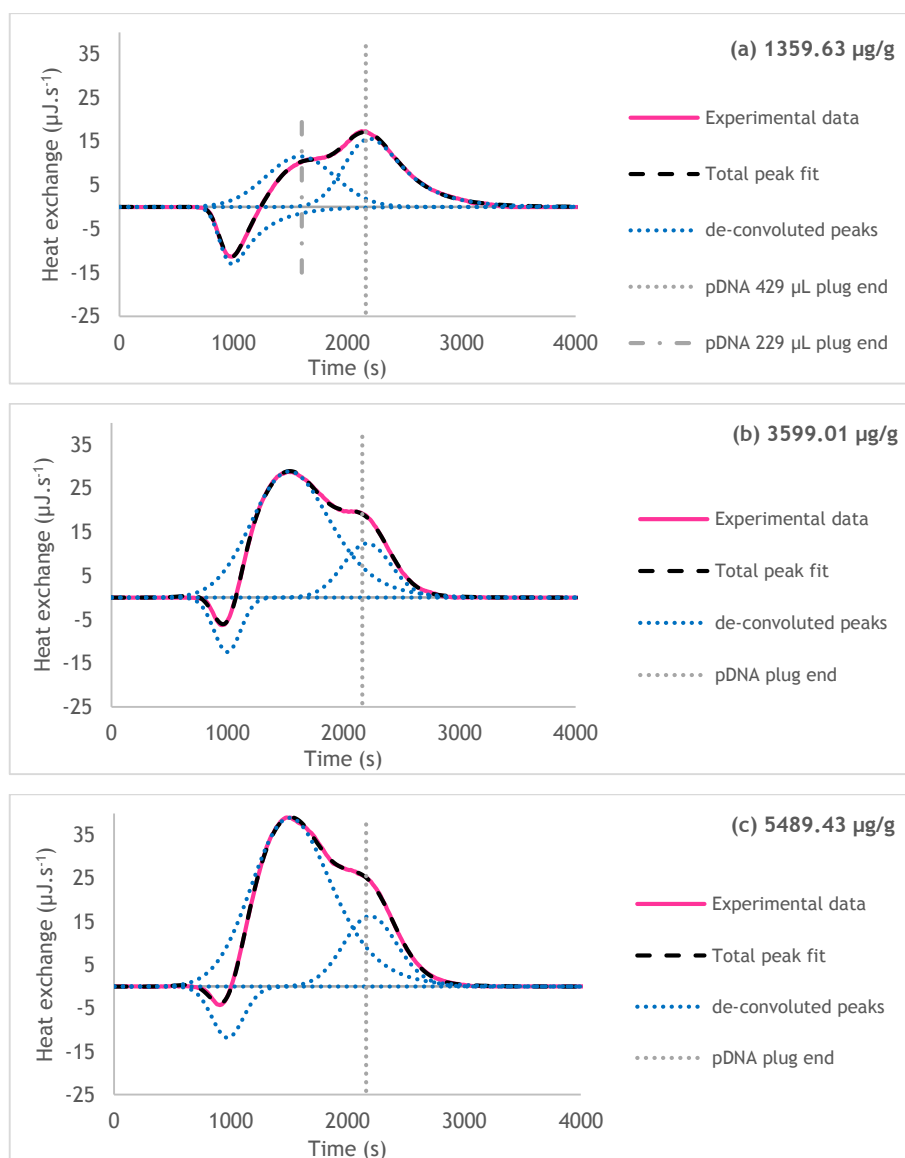


Figure 3.3.7 - PeakFIT de-convolution of thermograms for ln pDNA adsorption onto FF Q-sepharose for different loading concentrations, using the 429 μL loop: (a) 1359.63 μg pDNA/g Q-sepharose; (b) 3599.01 μg pDNA/g Q-sepharose; (c) 5489.43 μg pDNA/g Q-sepharose.

As stated above, the use of the 429 μL loop changes the profile of the heat signal and increases the whole interaction time, leading to a change in the magnitude of the heat signal and in the time at which each event took place. Additionally, the transition from a pulse to a continuous feed of ln pDNA into the packed cell also has influence in the sub-processes involved in the adsorption mechanism. This phenomenon is due to the fact that after the first 171 μL (cell volume) of the injected sample flow through the column, another 258 μL still have to pass through the column, interfering in the equilibrium already reached by the bound molecules. This mode of operation approaches the volume overloading used in some preparative chromatographic applications. In this case, to analyze the thermograms, it should be considered

another sub-process in the mechanism proposed by Yamamoto and co-workers (2001) that is related with the interaction between the bound pDNA molecules and the free pDNA molecules in the feed solution. Despite of some repulsion between these molecules, this interaction promotes the reorientation and the secondary adsorption of already bound biomolecules, leaving free space for pDNA in solution to adsorb. This is further supported considering the thermogram obtained in the linear zone of the isotherm, using the 429 μL loop (**Figure 3.3.7 a**) and observing the heat signal until around 1680 s (where the 229 μL loop pDNA plug ends) it can be seen that the profile of the peak is similar to the profile obtained with the 229 μL loop (**Figure 3.3.2**). After that, the adsorption enters in the volume overloading process and the heat signal magnitude increases until the end of the pDNA plug. This increase in the magnitude, as previous stated, may be due the secondary adsorption of the bound biomolecules in addition with the adsorption of more molecules.

Considering heat signals obtained in the transition and in the overloaded zones of the isotherm (**Figure 3.3.7 b and c**) and comparing them with a signal obtained in the linear zone (**Figure 3.3.7 a**), the relative magnitude of the first exothermic event to the second exothermic event seems to be related to the quantity of molecules present in the cell at the same time and interacting with the adsorbent. The first exothermic event presents a higher magnitude when compared to the second event under linear adsorption conditions, and this tendency is reversed for loadings in the transition and overloaded isotherm zones, thus suggesting its relation with the quantity of the pDNA molecules, as stated above. The observed behavior may be due to the fact that in the transition and overloaded zone, the high quantity of molecules does not favor the reorientation process, indeed from **Table 3.3.3** we can see that the enthalpy of adsorption of the first exothermic heat remains constant while its value for the second exothermic heat suffers a great decrease.

Table 3.3.4 presents the heats for \ln pDNA adsorption onto FF Q-sepharose, using different loops and considering the de-convoluted thermograms from the heat signals presented in **Figures 3.3.1 - 3.3.4**.

Figure 3.3.8 a presents the enthalpy changes (endothermic, exothermic and net heats divided by the pDNA adsorbed mass) for the \ln pDNA adsorption onto FF Q-sepharose, using the 30 and the 229 μL loops and considering the heat signals obtained from de-convolution. In this case, according to the loading concentrations, the enthalpies of adsorption correspond to the linear zone of the isotherm. **Figure 3.3.8 b** represents a “zoom in” of **Figure 3.3.8 a**. **Figure 3.3.8 c** also presents the adsorption enthalpies, but considering the thermograms obtained using the 429 μL loop, meaning that a volume overloading is being performed. In this case, pDNA loading concentration are in linear, transition and overloaded zones of the isotherm.

Table 3.3.4 - Heat of adsorption for ln pDNA adsorption onto FF Q-sepharose using different loops.

Loop (μL)	pDNA mass feed (μg)	pDNA loading ($\mu\text{g/g}$)	Endothermic Peak ($\text{mJ}/\mu\text{g}$)	Exothermic Peaks ($\text{mJ}/\mu\text{g}$)			Net heat of adsorption ($\text{mJ}/\mu\text{g}$)
			ΔH^{I}	ΔH^{II}	ΔH^{III}	$\Delta H^{\text{II}} + \Delta H^{\text{III}}$	ΔH^{Total}
30	0.27	12.55	1.160	-3.912	0	-3.912	-2.752
	1.17	53.35	2.164	-3.451	0	-3.451	-1.287
	2.43	111.23	1.049	-1.839	0	-1.839	-0.790
229	13.51	576.58	0.557	-0.832	0	-0.832	-0.275
	20.68	820.41	0.197	-0.512	0	-0.512	-0.315
	31.72	1222.50	0.232	-0.465	0	-0.465	-0.233
429	57.92	1359.63	0.189	-0.293	-0.363	-0.656	-0.467
	87.73	3599.01	0.045	-0.321	-0.082	-0.403	-0.358
	203.78	5489.43	0.033	-0.287	-0.077	-0.364	-0.331
1000	111.17	1830.54	0.465	-0.613	-0.209	-0.822	-0.357
	188.50	3884.83	0.060	-0.156	-0.165	-0.321	-0.261

$$\Delta H^{\text{Total}} = \Delta H^{\text{I}} + \Delta H^{\text{II}} + \Delta H^{\text{III}}$$

Considering the net heat of adsorption (sum of all contribution to heat), **Table 3.3.4** and **Figure 3.3.8**, the overall adsorption process is enthalpically driven, once it is exothermic for all the studied conditions, as expected for an anion-exchange interaction (Silva et al., 2014).

For the lower loading concentration, as pDNA loading increases the net heat of adsorption becomes more positive (**Figures 3.3.8 a and b**). Under these conditions, both endothermic and exothermic enthalpies decrease in magnitude. Endothermic heat major contribution was assumed to be water molecules and ion release from the pDNA and adsorbent surfaces. As the loading increases, each pDNA molecule foot print on the adsorbent surface may decrease in order to accommodate more molecules, thus less water molecules and ions need to be removed in the binding process, leading to a decrease of the endothermic heat signal.

Exothermic heat was assumed to result from the interaction process between the pDNA and from secondary adsorption of already adsorbed molecules. The decrease in the magnitude of the exothermic heat with the increase of the loading concentration is expected, as a higher repulsion between adsorbed molecules is observed.

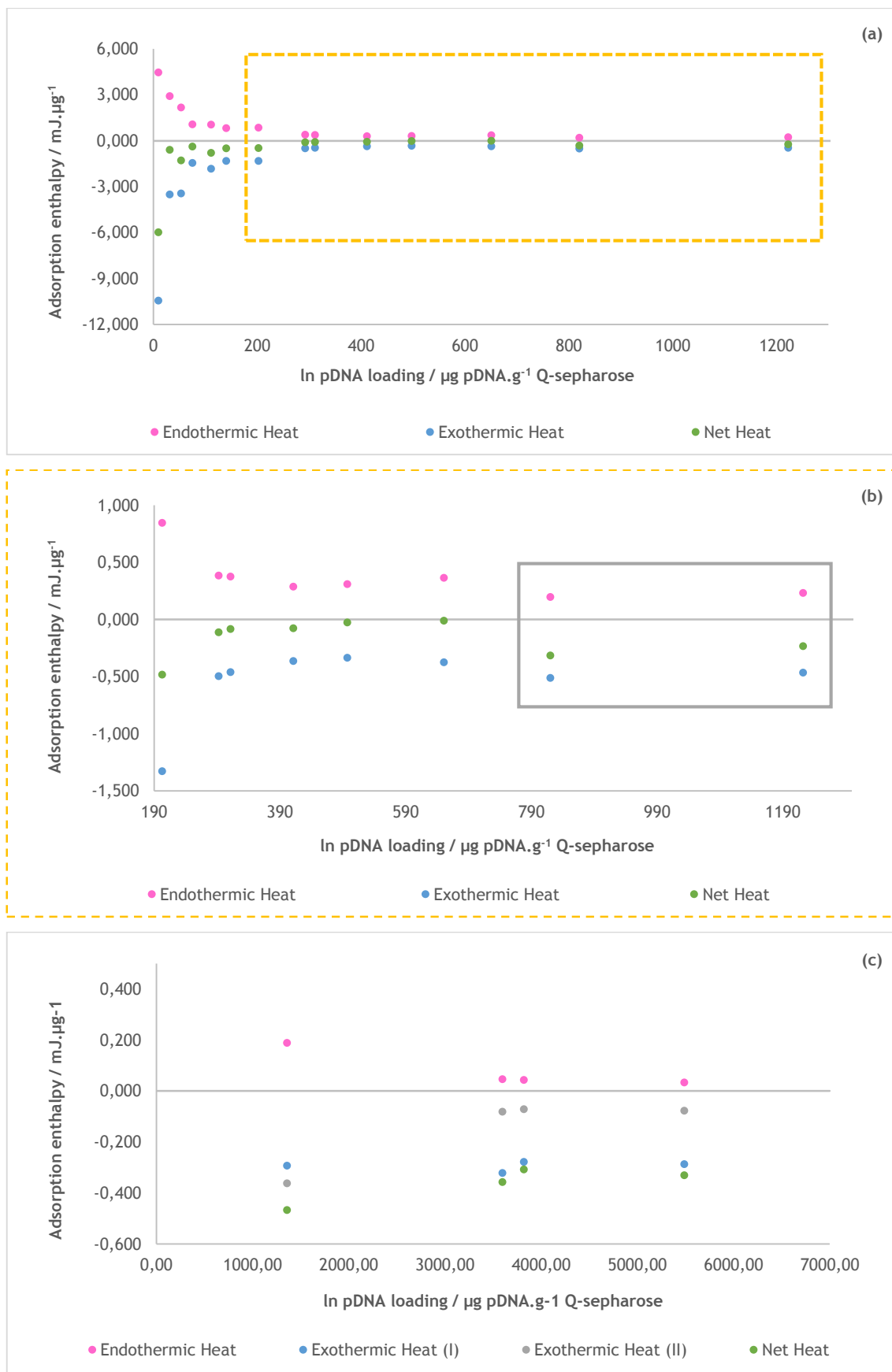


Figure 3.3.8 - Enthalpy of ln pDNA adsorption onto FF Q-sepharose using (a): 30 and 229 μL loops; (b) “zoom-in” of (a); (c) 429 and 1000 μL loops.

Considering **Figure 3.3.8 b**, highlighted points seems to be shifted, this is explained by the fact that these points were obtained using the 229 μL loop while the remaining ones were obtained with the 30 μL loop. As already discussed, the differences in the heat signal magnitude occur due to the increase in biomolecule resident time at the system, which gives more time for the equilibrium establishment (Silva et al., 2014).

Under overloaded conditions, the net heat of adsorption appears to be constant (**Figure 3.3.8 c**), which is expected as the monolayer capacity has been already reached (Silva et al., 2014).

3.4. Isothermal Titration Microcalorimetry (ITM)

Isothermal Titration Microcalorimetry (ITM) was performed to obtain further understanding of the global heat involved in the ln pDNA (pVAX1-LacZ) adsorption onto FF Q-sepharose. ITM heat signals were measured in the microcalorimeter fed-batch cell, adding the pDNA solution to the adsorbent suspended in the same buffer used in the pDNA solution. Data has been collected under linear adsorption conditions.

ITM results (**Figure 3.4.1 line A**) revealed heat signal for the ln pDNA adsorption onto FF Q-sepharose, in the linear zone of the isotherm, is characterized by an exothermic peak followed by an endothermic peak. Before doing the analysis of these results it is important to know if the dilution of the pDNA in the fed-batch cell has influence in the global heat signal. Thus, an experiment was performed where no adsorbent was introduced in the cell (the pDNA was injected in a cell filled only with buffer). Results from this experiment (**Figure 3.4.1 line B**) revealed that the pDNA dilution heat is characterized by a first exothermic peak followed by and endothermic peak.

Considering the heat signal obtained in the dilution experiment (**Figure 3.4.1 line B**) the first exothermic peak observed in the adsorption experiment (**Figure 3.4.1 line A**) seem to be related to the pDNA dilution in the fed-batch cell. Thus the global heat of adsorption of ln pDNA onto FF Q-sepharose, in the linear zone of the isotherm, is endothermic. These results are consistent with the FMC results obtained for the linear zone of the isotherm, using the 30 μL loop, where the endothermic heat signal was associated to the desolvation process (water molecules and ions release).

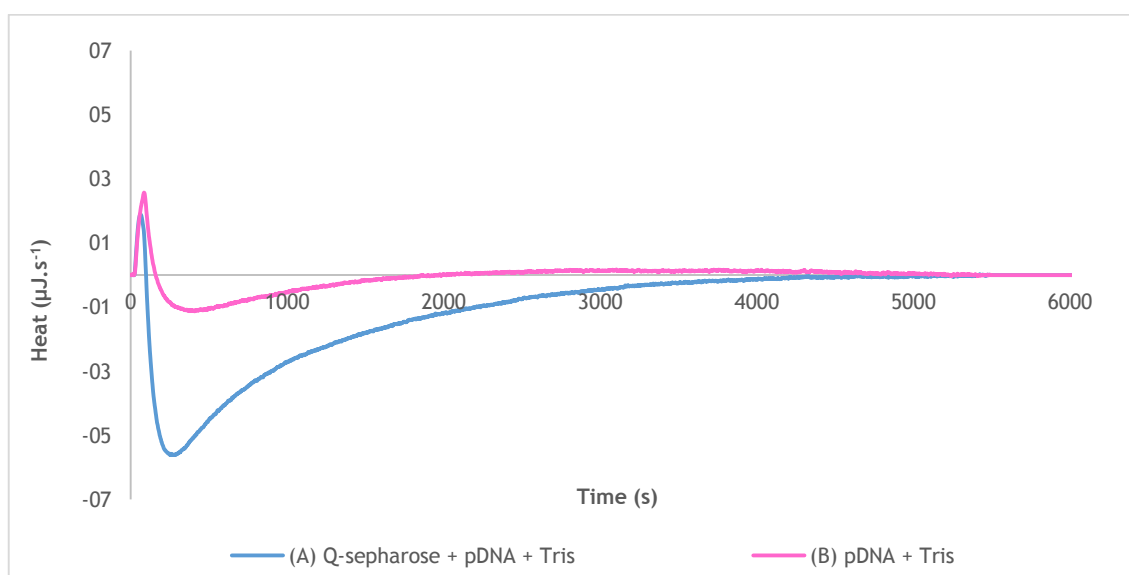


Figure 3.4.1 - Isothermal titration heat signals for: (A) ln pDNA adsorption onto FF Q-sepharose; (B) ln pDNA heat of dilution.

4. Conclusions and future work

Considering the great potential of pDNA as a therapeutic molecule, innumerous studies have been performed in order to produce and purify this biomolecule (Ghanem et al., 2013; Ginn et al., 2013; Sousa et al., 2009). Likewise as for any other biomolecule used in therapeutic fields, the pDNA production and purification requires the compliance of the guidelines from the regulatory agencies. Moreover, this processes ought to be scaled up to industrial scale and in this case economic issues have to be always taken into account.

Anion-exchange chromatography has been successfully used in pDNA purification (Ferreira et al., 2000; Ferreira, 2005; Ghanem et al., 2013; Sousa et al., 2009). However, the mechanisms involved in the pDNA separation, using anion-exchange chromatographic supports, are still not completely understood. Taking into account, the already proven ability of Flow Microcalorimetry (FMC) in the understanding of the driving forces, mechanisms and kinetics of biomolecules adsorption onto several chromatographic supports (Dias-Cabral et al., 2003; Katiyar et al., 2010; Ornelas et al., 2013; Silva et al., 2014; Thrash and Pinto, 2002, 2001; Thrash et al., 2004) this study used FMC as a central technique to understand the adsorption mechanism of ln pDNA (pVAX1-LacZ) onto the anion-exchange support Fast Flow Q-sepharose. Furthermore static binding capacity, Isothermal Titration Microcalorimetry (ITM) and fast performance chromatography were accomplished to obtain a better understanding of the adsorption mechanism.

Static binding capacity studies revealed that the mechanism of ln pDNA adsorption onto Q-sepharose follows a Langmuir-type isotherm profile (Bellot and Condoret, 1993; Langmuir, 1918). Values of pDNA adsorbed concentration above 4000 $\mu\text{g pDNA.g}^{-1}$ Q-sepharose were considered in the overloaded zone of the isotherm.

Flow Microcalorimetry (FMC) experiments were performed to understand the underlying mechanism of pDNA adsorption onto Q-sepharose, considering linear, transition and overloaded conditions, through a pulse injection or a continuous feed. All obtained thermograms comprised a first endothermic peak followed by an exothermic peak which, in some cases (volume overloading, 429 and 1000 μL injection loops), resulted from overlapped peaks. Thermograms obtained with a pulse injection (30 and 229 μL loops) have similar heat signal profiles and the increase in the injection volume from 30 to 229 μL resulted in an increase in the time of the whole interaction, leading to change in the magnitude of the heat signal and in time at which each event took place. The same was verified for thermograms obtained with a continuous feed (429 and 1000 μL loops). However, when a thermogram obtained from a pulse injection was compared with a thermogram obtained from a continuous feed differences were found not only

in the heat signal magnitude and in the time at which each event took place, but also in the peak profile. The presence of different peaks in a thermogram suggested the existence of different events during the adsorption process. Thermograms were analyzed considering the mechanism proposed by Yamamoto and co-workers (Lin et al., 2001). Endothermic heat major contributor was suggested to be the desolvation process, including water molecules and ions release, while exothermic heats were related to the interaction (electrostatic attraction) between λ pDNA and FF Q-sepharose and also to the secondary adsorption of already adsorbed pDNA molecules (biomolecules reorientation).

Furthermore, FMC revealed that the overall adsorption process is exothermic, as expected for an anion-exchange interaction. For the lower loading concentrations, as pDNA loading increases the net heat of adsorption became more positive. Under these conditions, both endothermic and exothermic enthalpies decreased in magnitude. As the loading increases, each pDNA molecule foot print on the adsorbent surface may decrease in order to accommodate more molecules, thus less water molecules and ions need to be removed in the binding process, leading to a decrease of the endothermic heat signal. The decrease in the magnitude of the exothermic heat with the increase of the loading concentration was expected, as a higher repulsion between adsorbed molecules is observed. Under overloaded conditions, the net heat of adsorption appears to be constant, which was expected as the monolayer capacity has been already reached (Silva et al., 2014). ITM results were consistent with the FMC results, and supported the fact that the major contribution of the desolvation process for the low loading pDNA concentrations. All these results confirm that flow microcalorimetry is a useful technique illustrating the underlying mechanism associated with pDNA adsorption and elucidating the role of non-specific effects in the establishment of the adsorptive process.

Future work will be accomplished using the same chromatographic support in order to understand the adsorption mechanism of the supercoiled isoform of the same pDNA. Despite being more complex, the supercoiled isoform is the more biologically active and because of that is most used in therapeutic applications (Ghanem et al., 2013; Sousa et al., 2009). Results from the linear and the supercoiled pDNA adsorption will be compared. If differences are found in their adsorption mechanisms, they may be explored in order to optimize the purification chromatographic methods.

Additionally, once Hydrophobic Interaction Chromatography (HIC) has shown its aptitude in the pDNA purification (Freitas et al., 2009; Raiado-Pereira et al., 2013), it will be interesting to perform the same studies using a hydrophobic interaction support. FMC results from anion-exchange and hydrophobic interaction will be compared in order to identify possible differences between the adsorption mechanisms characteristics for each chromatographic technique. Moreover, the use of FMC to evaluate the adsorption mechanisms of novel chromatographic supports will be a useful tool to their characterization.

References

- Bellot, J.C., Condoret, J.S., 1993. Review Modelling of Liquid Chromatography Equilibria. *Process Biochem.* 28, 365-376.
- Blaschke, T., Varon, J., Werner, A., Hasse, H., 2011. Microcalorimetric study of the adsorption of PEGylated lysozyme on a strong cation exchange resin. *J. Chromatogr. A* 1218, 4720-4726.
- Blaschke, T., Werner, A., Hasse, H., 2013. Microcalorimetric study of the adsorption of native and mono-PEGylated bovine serum albumin on anion-exchangers. *J. Chromatogr. A* 1277, 58-68.
- Bowen, W.R., Pan, L.-C., 1997. Ion Exchange of Bovine Serum Albumin at a Natural Organic Anion Exchanger: Thermodynamics and Energetics. *J. Colloid Interface Sci.* 189, 328-336.
- Carta, G., Jungbauer, A., 2010. *Protein Chromatography: Process Development and Scale Up*.
- Chen, W., Lin, M., Lin, P., Tasi, P., Chang, Y., Yamamoto, S., 2007. Studies of the interaction mechanism between single strand and double-strand DNA with hydroxyapatite by microcalorimetry and isotherm measurements. *Colloids Surfaces A* 295, 274-283.
- Dias-Cabral, a. C., Queiroz, J. a., Pinto, N.G., 2003. Effect of salts and temperature on the adsorption of bovine serum albumin on polypropylene glycol-Sepharose under linear and overloaded chromatographic conditions. *J. Chromatogr. A* 1018, 137-153.
- Dieterle, M., Blaschke, T., Hasse, H., 2008. Microcalorimetric study of adsorption of human monoclonal antibodies on cation exchange chromatographic materials. *J. Chromatogr. A* 1205, 1-9.
- Esquibel-King, M.A., Dias-Cabral, A.C., Queiroz, J.A., Pinto, N.G., 1999. Study of hydrophobic interaction adsorption of bovine serum albumin under overloaded conditions using flow microcalorimetry. *J. Chromatogr. A* 865, 111-122.
- Fernández, L.L., Montes-Bayón, M., González, E.B., Sierra, L.M., Sanz-Medel, A., Bettmer, J., 2011. Initial studies on quantitative DNA induced oxidation by gel electrophoresis (GE)-ICP-MS. *J. Anal. At. Spectrom.* 26, 195-200.
- Ferreira, G.N., Cabral, J.M., Prazeres, D.M., 2000a. Studies on the batch adsorption of plasmid DNA onto anion-exchange chromatographic supports. *Biotechnol. Prog.* 16, 416-424.

- Ferreira, G.N., Monteiro, G. a, Prazeres, D.M., Cabral, J.M., 2000b. Downstream processing of plasmid DNA for gene therapy and DNA vaccine applications. *Trends Biotechnol.* 18, 380-388.
- Ferreira, G.N.M., 2005. Chromatographic Approaches in the Purification of Plasmid DNA for Therapy and Vaccination. *Chem. Eng. Technol.* 28, 1285-1294.
- Freitas, S.S., Santos, J. a. L., Prazeres, D.M.F., 2009. Plasmid purification by hydrophobic interaction chromatography using sodium citrate in the mobile phase. *Sep. Purif. Technol.* 65, 95-104.
- G.E. Healthcare, 2007. Q Sepharose Fast Flow instructions. Instr. 71-5009-64 AE.
- Gallant, S.R., Kundu, A., Cramer, S.M., 1995. Modeling non-linear elution of proteins in ion-exchange chromatography. *J. Chromatogr. A* 702, 125-142.
- Ghanem, A., Healey, R., Adly, F.G., 2013. Current trends in separation of plasmid DNA vaccines: a review. *Anal. Chim. Acta* 760, 1-15.
- Gill, D.S., Roush, D.J., Shick, K. a, Willson, R.C., 1995. Microcalorimetric characterization of the anion-exchange adsorption of recombinant cytochrome b5 and its surface-charge mutants. *J. Chromatogr. A* 715, 81-93.
- Ginn, S., Alexander, I., Edelstein, M., Abedi, M., Wixon, J., 2013. Gene therapy clinical trials worldwide to 2012-an update. *J. Gene Med.* 15, 65-77.
- Katiyar, A., Thiel, S.W., Gulianti, V. V, Pinto, N.G., 2010. Investigation of the mechanism of protein adsorption on ordered mesoporous silica using flow microcalorimetry. *J. Chromatogr. A* 1217, 1583-1588.
- Kelly, W.J., 2003. Perspectives on plasmid-based gene therapy : challenges for the product and the process. *Biotechnol. Appl. Biochem.* 37, 219-223.
- Kim, J., Desch, R.J., Thiel, S.W., Gulianti, V. V, Pinto, N.G., 2011a. Energetics of protein adsorption on amine-functionalized mesostructured cellular foam silica. *J. Chromatogr. A* 1218, 7796-7803.
- Kim, J., Desch, R.J., Thiel, S.W., Gulianti, V. V, Pinto, N.G., 2011b. Energetics of lysozyme adsorption on mesostructured cellular foam silica: effect of salt concentration. *J. Chromatogr. A* 1218, 6697-6704.

- Kim, J., Desch, R.J., Thiel, S.W., Guliants, V. V., Pinto, N.G., 2013. Energetics of biomolecule adsorption on mesostructured cellular foam silica. *Microporous Mesoporous Mater.* 170, 95-104.
- Korfhagen, J., Dias-Cabral, A.C., Thrash, M.E., 2010. Nonspecific Effects of Ion Exchange and Hydrophobic Interaction Adsorption Processes. *Sep. Sci. Technol.* 45, 2039-2050.
- Langmuir, I., 1918. The adsorption of gases on plane surfaces of glass, mica and platinum. *J. Am. Chem. Soc.* 40, 1361-1403.
- Li, L., Saade, F., Petrovsky, N., 2012. The future of human DNA vaccines. *J. Biotechnol.* 162, 171-182.
- Lin, F., Chen, W., Hearn, M.T.W., 2002. Thermodynamic analysis of the interaction between proteins and solid surfaces : application to liquid chromatography. *J. Mol. Recognit.* 15, 55-93.
- Lin, F.Y., Chen, C.S., Chen, W.Y., Yamamoto, S., 2001. Microcalorimetric studies of the interaction mechanisms between proteins and Q-sepharose at pH near the isoelectric point (pI) effects of NaCl concentration, pH value, and temperature. *J. Chromatogr. A* 912, 281-289.
- Ornelas, M., Loureiro, D., Araújo, M.J., Marques, E., Dias-Cabral, C., Azenha, M., Silva, F., 2013. Synthesis of glycylglycine-imprinted silica microspheres through different water-in-oil emulsion techniques. *J. Chromatogr. A* 1297, 138-145.
- Perkins, T.W., Mak, D.S., Root, T.W., Lightfoot, E.N., 1997. Protein retention in hydrophobic interaction chromatography: modeling variation with buffer ionic strength and column hydrophobicity. *J. Chromatogr. A* 766, 1-14.
- Phillips, J.M., Pinto, N.G., 2004. Calorimetric investigation of the adsorption of nitrogen bases and nucleosides on a hydrophobic interaction sorbent. *J. Chromatogr. A* 1036, 79-86.
- Pierce, M.M., Raman, C.S., Nall, B.T., 1999. Isothermal titration calorimetry of protein-protein interactions. *Methods* 19, 213-221.
- Rabe, M., Verdes, D., Seeger, S., 2011. Understanding protein adsorption phenomena at solid surfaces. *Adv. Colloid Interface Sci.* 162, 87-106.
- Raiado-Pereira, L., Prazeres, D.M.F., Mateus, M., 2013. Impact of plasmid size on the purification of model plasmid DNA vaccines by phenyl membrane adsorbers. *J. Chromatogr. A* 1315, 145-151.

- Raje, P., Pinto, N.G., 1997. Combination of the steric mass action and non-ideal surface solution models for overload protein ion-exchange chromatography. *J. Chromatogr. A* 760, 89-103.
- Raje, P., Pinto, N.G., 1998. Importance of heat of adsorption in modeling protein equilibria for overloaded chromatography. *J. Chromatogr. A* 796, 141-156.
- Silva, F., Passarinha, L., Sousa, F., Queiroz, J.A., Domingues, F.C., 2009. Influence of Growth Conditions on Plasmid DNA Production. *J. Microbiol. Biotechnol.* 19, 1408-1414.
- Silva, G.L., Marques, F.S., Thrash, M.E., Dias-Cabral, A.C., 2014. Enthalpy contributions to adsorption of highly charged lysozyme onto a cation-exchanger under linear and overloaded conditions. *J. Chromatogr. A* 1352, 46-54.
- Smith, C.R., DePrince, R.B., Dackor, J., Weigl, D., Griffith, J., Persmark, M., 2007. Separation of topological forms of plasmid DNA by anion-exchange HPLC: shifts in elution order of linear DNA. *J. Chromatogr. B* 854, 121-127.
- Sousa, F., Passarinha, L., Queiroz, J.A., 2009. Biomedical application of plasmid DNA in gene therapy: a new challenge for chromatography. *Biotechnol. Genet. Eng. Rev.* 26, 83-116.
- Thrash, M.E., Phillips, J.M., Pinto, N.G., 2004. An Analysis of the Interactions of BSA with an Anion-Exchange Surface Under Linear and Non-Linear Conditions. *Adsorpt. Int. Adsorpt. Soc.* 10, 299-307.
- Thrash, M.E., Pinto, N.G., 2001. Flow microcalorimetric measurements for bovine serum albumin on reversed-phase and anion-exchange supports under overloaded conditions. *J. Chromatogr. A* 908, 293-299.
- Thrash, M.E., Pinto, N.G., 2002. Characterization of enthalpic events in overloaded ion-exchange chromatography. *J. Chromatogr. A* 944, 61-68.